steric and electronic effects that determine product distribution.[18] We are continuing further investigations of these processes in related systems.

Acknowledgment. We gratefully acknowledge the Petroleum Research Fund and a Cottrell grant from the Research Corp. for financial support. We thank Johnson-Matthey Co. for a loan of iridium salts.

(18) Bergman and co-workers have observed a similar stereoselectivity in methylene/hydride site exchange in a heterodinuclear (Ta/Pt) system.[3a]

Supplementary Material Available: Tables of anisotropic temperature factors and bond lengths and bond angles for **2** (3 pages); a listing of observed and calculated structure factors (14 pages). Ordering information is given on any current masthead page.

The Facile Transformation of a Hydrido Alkynyl to Vinylidene Ligand on a Tetranuclear Metal Framework, a Process Involving a Reversible Skeletal Rearrangement. Syntheses and Crystal Structures of the Triruthenium–Platinum Clusters $Ru_3Pt(\mu\text{-}H)\{\mu_4\text{-}\eta^2\text{-}C{\equiv}C(t\text{-}Bu)\}(CO)_9(C_8H_{12})$, $Ru_3Pt(\mu\text{-}H)\{\mu_4\text{-}\eta^2\text{-}C{\equiv}C(t\text{-}Bu)\}(CO)_9(Ph_2P(CH_2)_2PPh_2)$, $Ru_3Pt(\mu_4\text{-}\eta^2\text{-}C{=}C(H)t\text{-}Bu)(CO)_9(Ph_2P(CH_2)_2PPh_2)$, and $[Ru_3Pt(\mu\text{-}H)(\mu_4\text{-}\eta^2\text{-}C{=}C(H)t\text{-}Bu)(CO)_9(Ph_2P(CH_2)_2PPh_2)]^+BF_4^-$

Paul Ewing and Louis J. Farrugia*

Department of Chemistry, The University, Glasgow, G12 8QQ, U.K.

Received September 21, 1988

Treatment of $R_3(\mu\text{-}H)\{\mu_3\text{-}\eta^2\text{-}C{\equiv}C(t\text{-}Bu)\}(CO)_9$ with $Pt(COD)_2$ (COD = cycloocta-1,5-diene) affords the tetranuclear alkynyl cluster $Ru_3Pt(\mu\text{-}H)\{\mu_4\text{-}\eta^2\text{-}C{\equiv}C(t\text{-}Bu)\}(CO)_9(COD)$ (**4**). Crystal data for **4**: monoclinic, space group $P2_1/n$; a = 11.283 (3), b = 17.843 (2), c = 13.625 (3) Å; β = 94.06 (2)°; V = 2736 (1) Å^3; Z = 4; final R (R_w) values 0.023 (0.029) for 3815 independent observed data ($I > 3.0\sigma(I)$). **4** has an "out-of-plane" spiked-triangular metal framework with a platinum atom bonded to an equilateral Ru_3 triangle via one Ru atom (Ru–Ru = 2.791 (1)–2.815 (1), Ru(2)–Pt = 2.645 (1) Å). The $\mu_4\text{-}\eta^2(\perp)$-alkynyl ligand is σ-bonded to the Pt atom and Ru(2) and asymmetrically π-bonded to the remaining two Ru atoms (Ru(1)–C(11) = 2.484 (5), Ru(3)–C(11) = 2.291 (5) Å), which are also bridged by a hydride. The Pt atom is asymmetrically chelated to a COD ligand, which is easily displaced by bis(diphenylphosphino)ethane (dppe) affording two complexes, the hydrido alkynyl $Ru_3Pt(\mu\text{-}H)\{\mu_4\text{-}\eta^2\text{-}C{\equiv}C(t\text{-}Bu)\}(CO)_9(dppe)$ (**6**) and the tautomeric vinylidene cluster $Ru_3Pt(\mu_4\text{-}\eta^2\text{-}C{=}C(H)t\text{-}Bu)(CO)_9(dppe)$ (**11**). Crystal data for **6**: monoclinic, space group $P2_1/n$; a = 13.867 (3), b = 17.725 (2), c = 17.429 (7) Å; β = 92.50 (2)°; V = 4280 (2) Å^3; Z = 4; final R (R_w) values 0.028 (0.032) for 5167 independent observed data ($I > 3.0\sigma(I)$). Crystal data for **11**: monoclinic, space group $C2/c$; a = 47.561 (5), b = 12.176 (2), c = 23.155 (10) Å; β = 118.27 (2)°; V = 11810 (6) Å^3; Z = 8; final R (R_w) values 0.048 (0.056) for 5865 independent observed data ($I > 2.5\sigma(I)$). Complex **6** has a similar Ru_3Pt core (Ru–Ru = 2.792 (1)–2.824 (1), Ru(3)–Pt = 2.681 (1) Å) and $\mu_4\text{-}\eta^2(\perp)$-alkynyl geometry to that found in **4**, except that this ligand is more symmetrically π-bonded to the two hydrido-bridged Ru atoms (Ru(1)–C(11) = 2.396 (6), Ru(2)–C(11) = 2.427 (6) Å). Complex **11** has a $\mu_4\text{-}\eta^2$-vinylidene ligand bonded to a butterfly Ru_3Pt core, with the Pt atom on a wingtip (Ru–Ru = 2.708 (2)–2.823 (2) Å; Pt–Ru = 2.730 (1), 2.792 (1) Å). The vinylidene moiety is σ-bonded to the Pt atom and to two Ru atoms and is π-bonded to the remaining Ru center. Complexes **6** and **11** readily interconvert in solution, with **11** being the thermodynamically favored product. This facile process involves a reversible skeletal rearrangement of the Ru_3Pt core, and kinetic studies imply an intramolecular mechanism. **11** is protonated by HBF_4 along a metal–metal edge, giving the cationic hydrido vinylidene cluster $[Ru_3Pt(\mu\text{-}H)(\mu_4\text{-}\eta^2\text{-}C{=}C(H)t\text{-}Bu)(CO)_9(dppe)]^+BF_4^-$ (**17**). Crystal data for **17**: triclinic, space group $P\bar{1}$; a = 10.189 (4), b = 14.329 (4), c = 15.596 (9) Å; α = 97.70 (4), β = 94.72 (4), γ = 98.75 (3)°; V = 2218 (2) Å^3; Z = 2, final R (R_w) values 0.035 (0.044) for 6293 independent observed data ($I > 3.0\sigma(I)$). The cluster core closely resembles that found in **11**, with a hydride ligand bridging the hinge Ru–Ru vector. Protonation of **6** occurs at the α-carbon of the acetylide affording the alkyne complex $[Ru_3Pt(\mu\text{-}H)(\mu_4\text{-}\eta^2\text{-}HC{\equiv}C(t\text{-}Bu))(CO)_9(dppe)]^+BF_4^-$ (**18**). **18** irreversibly isomerizes to **17** in solution.

Introduction

There is continuing interest in the structural chemistry[1] and reactivity[2,3] of unsaturated hydrocarbyl ligands that are coordinated to several metal atom sites, since these systems may provide models for reactive species and in-

(1) (a) Sappa, E.; Tiripicchio, A.; Braunstein, P. *Coord. Chem. Rev.* **1985**, *65*, 219. (b) Nast, R. *Coord. Chem. Rev.* **1982**, *47*, 89. (c) Raithby, P. R.; Rosales, M. J. *Adv. Inorg. Chem. Radiochem.* **1985**, *29*, 169. (d) Sappa, E.; Tiripicchio, A.; Braunstein, P. *Chem. Rev.* **1983**, *83*, 203. (e) Carty, A. J. *Pure Appl. Chem.* **1982**, *54*, 113. (f) Herrmann, W. A. *Adv. Organomet. Chem.* **1982**, *20*, 160.

(2) (a) Adams, R. D.; Horváth, I. T. *Prog. Inorg. Chem.* **1985**, *33*, 127. (b) Deeming, A. J. In *Transition Metal Clusters*; Johnson, B. F. G., Ed.; Wiley: Chichester, 1980; pp 391–469. (c) Lavigne, G.; Kaesz, H. D. In *Studies in Surface Science and Catalysis*; Gates, B. C., Guczi, L., Knözinger, H., Eds.; Elsevier: Amsterdam, 1986; Vol. 29, Chapter 4, pp 43–88. (d) Bradley, J. S. In *Metal Clusters*; Moskovits, M., Ed.; Wiley: Chichester, 1986; Chapter 5, pp 105–130.

0276-7333/89/2308-1246$01.50/0

termediates in heterogeneous catalysis.[4] Multisite bound alkynyl ligands are known to be susceptible toward nucleophilic attack,[5,6] and such reactivity can be used to form new C–C bonds on the cluster template.[1e,5,7] One well-established series of clusters containing such ligands are the complexes $M_3(\mu\text{-H})(\mu_3\text{-}\eta^2\text{-C}{\equiv}\text{CR})(\text{CO})_9$ (M = Ru, Os), of which structurally characterized examples include **1a** (M = Os, R = CF_3)[8] and **2a** (M = Ru, R = *t*-Bu).[9] A

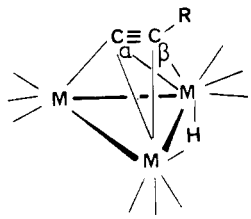

1, M = Os ; **2**, M = Ru

theoretical study by Granozzi et al.[10] on **2b** (R = Me) indicated that under charge control the α-carbon atom was the likely site of nucleophilic attack, as this center bears a slight positive charge. Since the LUMO is of M–M σ-antibonding character and has no contribution from the alkynyl ligand while the HOMO is essentially a M–M σ-bonding MO with minimal alkynyl character,[10] the site specificity of nucleophilic attack under orbital control is likely to be directed toward the metal atoms. In practice, however, the situation is more complex; for instance Deeming and co-workers[11] have shown that although **1b** (R = H) reacts with nucleophiles predominantly at the C_α site, attack at the C_β site is also feasible.

We have recently reported the synthesis and X-ray structure of the tetranuclear alkynyl cluster $Os_3Pt(\mu\text{-H})(\mu_4\text{-}\eta^2\text{-C}{\equiv}\text{CPh})(\text{CO})_{10}(PCy_3)$ (**3**, Cy = c-C_6H_{11}), which is formed by treatment of the unsaturated triosmium–platinum cluster $Os_3Pt(\mu\text{-H})_2(\text{CO})_{10}(PCy_3)$ with LiC≡CPh followed by protonation.[12] Complex **3** has an "out-of-plane" spiked-triangular Os_3Pt core, with the alkynyl ligand adopting an asymmetric $\mu_4\text{-}\eta^2(\perp)$ coordination mode. Formally this complex may also be thought of as arising from the addition of a PtL_2 fragment [L_2 = (CO)(PCy_3)] to the alkynyl complex **1c** (R = Ph), i.e. an addition involving attack at C_α by a transition-metal-centered nucleophile. Herein we describe the reaction of complex **2a**, a triruthenium analogue of **1c**, with $Pt(COD)_2$ (COD = cycloocta-1,5-diene), which results in direct addition of a Pt(COD) fragment to the C_α of the alkynyl. The resultant complex has a $\mu_4\text{-}\eta^2$-alkynyl geometry similar to that found in **3**.

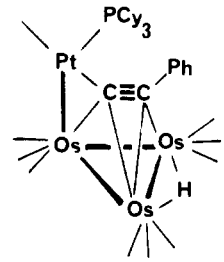

3

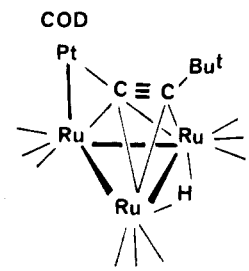

4

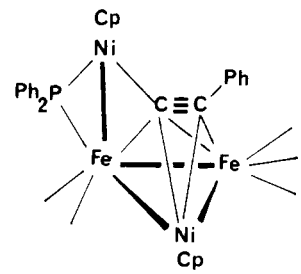

5

Results and Discussion

Synthesis and Spectroscopic Data on $Ru_3Pt(\mu\text{-H})\{\mu_4\text{-}\eta^2\text{-C}{\equiv}\text{C}(t\text{-Bu})\}(\text{CO})_9(\text{COD})$ (4). Treatment of a toluene solution of **2a** with an equimolar amount of $Pt(COD)_2$ results in a dark brown solution, which on workup affords reasonable isolated yields (50–60%) of the bright orange crystalline complex $Ru_3Pt(\mu\text{-H})\{\mu_4\text{-}\eta^2\text{-C}{\equiv}\text{C}(t\text{-Bu})\}(\text{CO})_9(\text{COD})$ (**4**). Solutions of complex **4** are quite air-sensitive and decompose slowly in the absence of small amounts of COD. The ^1H NMR spectrum at 295 K showed singlet resonances at δ 1.28 and −19.23 (J(Pt–H) = 6.4 Hz) due to the *t*-Bu and Ru(μ-H)Ru protons, respectively, and three broad bands at δ 6.02 (2 H), 5.35 (2 H), and 1.73 (8 H) due to the coordinated COD ligand. The olefinic signals (δ 6.02 and 5.35) were too broad to display ^{195}Pt satellites but at 233 K were considerably sharper and showed resolvable ^{195}Pt coupling (J(Pt–H) = 49 and 71 Hz respectively). This result indicates that **4** has two sets of inequivalent olefinic protons which exchange at room temperature due to a "ring whizzing" or

(3) For some recent papers on the reactivity of cluster-coordinated unsaturated organic ligands see: (a) Henrick, K.; McPartlin, M.; Iggo, J. A.; Kemball, A. C.; Mays, M. J.; Raithby, P. R. *J. Chem. Soc., Dalton Trans.* **1987**, 2669. (b) Cowie, A. G.; Johnson, B. F. G.; Lewis, J. *Ibid.* **1987**, 2839. (c) Deeming, A. J.; Arce, A. J.; De Sanctis, Y.; Bates, B. A.; Hursthouse, M. B. *Ibid.* **1987**, 2935. (d) Delgado, E.; Garcia, M. E.; Jeffery, J. C.; Sherwood, P.; Stone, F. G. A. *Ibid.* **1988**, 207. (e) Puga, J.; Arce, A.; Sanchez-Delgado, R. A.; Ascanio, J.; Adriollo, A.; Braga, D.; Grepioni, F. *Ibid.* **1988**, 913. (f) Hogarth, G.; Kayser, F.; Knox, S. A. R.; Morton, D. A. V.; Orpen, A. G.; Turner, M. L. *J. Chem. Soc., Chem. Commun.* **1988**, 358. (g) Dutta, T. K.; Meng, X.; Vites, J. C.; Fehlner, T. P. *Organometallics* **1987**, *6*, 2191. (h) Bassner, S. L.; Morrison, E. D.; Geoffroy, G. L.; Rheingold, A. L. *Ibid.* **1987**, *6*, 2207. (i) Han, S.-H.; Geoffroy, G. L.; Rheingold, A. L. *Ibid.* **1987**, *6*, 2380. (j) Nuel, D.; Mathieu, R. *Ibid.* **1988**, *7*, 16. (k) Suades, J.; Dahan, F.; Mathieu, R. *Ibid.* **1988**, *7*, 47. (l) Nucciarone, D.; Taylor, N. J.; Carty, A. J.; Tiripicchio, A.; Tiripicchio Camellini, M.; Sappa, E. *Ibid.* **1988**, *7*, 118. (m) Nucciarone, D.; Taylor, N. J.; Carty, A. J. *Ibid.* **1988**, *7*, 127. (n) Crespi, A. M.; Went, M. J.; Sunshine, S. S.; Shriver, D. F. *Ibid.* **1988**, *7*, 214. (o) Casey, C. P.; Crocker, M.; Vosejpka, P. C.; Fagan, P. J.; Marder, S. R.; Gohdes, M. A. *Ibid.* **1988**, *7*, 670. (p) Sailor, M. J.; Sabat, M.; Shriver, D. F. *Ibid.* **1988**, *7*, 728. (q) Aradi, A. A.; Grevels, F.-W.; Krüger, C.; Raabe, E. *Ibid.* **1988**, *7*, 812. (r) Ching, S.; Holt, E. M.; Kolis, J. W.; Shriver, D. F. *Ibid.* **1988**, *7*, 892. (s) Casey, C. P.; Vosejpka, P. C. *Ibid.* **1988**, *7*, 934. (t) Adams, R. D.; Babin, J. E. *Ibid.* **1988**, *7*, 963. (u) Hriljac, J. A.; Shriver, D. F. *J. Am. Chem. Soc.* **1987**, *109*, 6010. (v) Sailor, M. J.; Brock, C. P.; Shriver, D. F. *Ibid.* **1987**, *109*, 6015. (w) Went, M. J.; Sailor, M. J.; Bogdan, P. L.; Brock, C. P.; Shriver, D. F. *Ibid.* **1987**, *109*, 6023. (x) Albiez, T.; Vahrenkamp, H. *Angew. Chem., Int. Ed. Engl.* **1987**, *26*, 572.

(4) (a) Muetterties, E. L.; Rhodin, T. N.; Band, E.; Brucker, C. F.; Pretzer, W. R. *Chem. Rev.* **1979**, *79*, 91. (b) Evans, J. *Chem. Soc. Rev.* **1981**, *10*, 159. (c) Somorjai, G. A. *Chem. Soc. Rev.* **1984**, *13*, 321. (d) Canning, N. D. S.; Madix, R. J. *J. Phys. Chem.* **1984**, *88*, 2437. (e) Koestner, R. J.; Van Hove, M. A.; Somorjai, G. A. *J. Phys. Chem.* **1983**, *87*, 203.

(5) Nucciarone, D.; MacLaughlin, S. A.; Taylor, N. J.; Carty, A. J. *Organometallics* **1988**, *7*, 106 and references therein.

(6) (a) Henrick, K.; McPartlin, M.; Deeming, A. J.; Hasso, S.; Manning, P. *J. Chem. Soc., Dalton Trans.* **1982**, 899. (b) Aime, S.; Deeming, A. J. *Ibid.* **1983**, 1807. (c) Aime, S.; Osella, D.; Arce, A. J.; Deeming, A. J.; Hursthouse, M. B.; Galas, A. M. R. *Ibid.* **1984**, 1981.

(7) MacLaughlin, S. A.; Johnson, J. P.; Taylor, N. J.; Carty, A. J.; Sappa, E. *Organometallics* **1983**, *2*, 352.

(8) Dawoodi, Z.; Mays, M. J.; Henrick, K. *J. Chem. Soc., Dalton Trans.* **1984**, 1769.

(9) Catti, M.; Gervasio, G.; Mason, S. A. *J. Chem. Soc., Dalton Trans.* **1977**, 2260.

(10) Granozzi, G.; Tondello, E.; Bertoncello, R.; Aime, S.; Osella, D. *Inorg. Chem.* **1983**, *22*, 744.

(11) Boyar, E.; Deeming, A. J.; Kabir, S. A. *J. Chem. Soc., Chem. Commun.* **1986**, 577.

(12) Ewing, P.; Farrugia, L. J. *J. Organomet. Chem.* **1987**, *320*, C47.

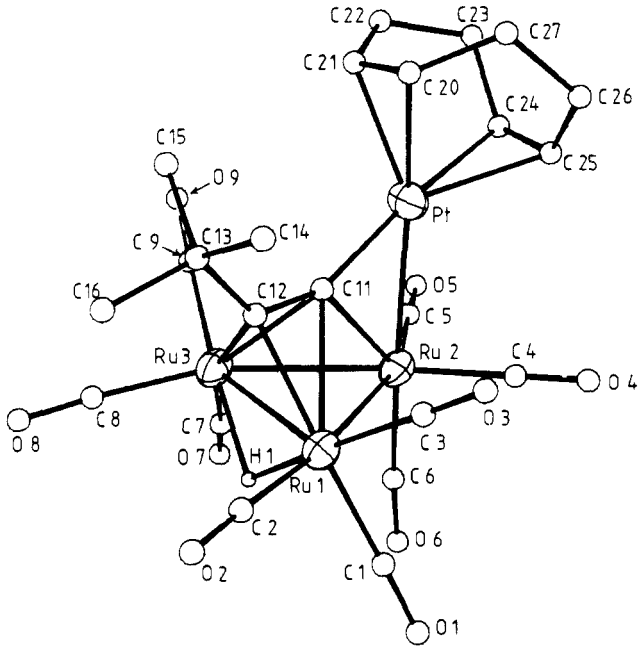

Figure 1. Molecular structure of the complex $Ru_3Pt(\mu\text{-}H)\{\mu_4\text{-}\eta^2\text{-}C{\equiv}C(t\text{-}Bu)\}(CO)_9(COD)$ (**4**).

Table I. Final Positional Parameters (Fractional Coordinates) with Esd's in Parentheses and Isotropic Thermal Parameters (Equivalent Isotropic Parameters U_{eq} for Anisotropic Atoms) for $Ru_3Pt(\mu\text{-}H)\{\mu_4\text{-}\eta^2\text{-}C{\equiv}C(t\text{-}Bu)\}(CO)_9(COD)$ (4)[a]

	x/a	y/b	z/c	U_{eq}, Å^2
Pt	0.54159 (2)	0.36222 (1)	0.27961 (1)	0.038
Ru(1)	0.87143 (4)	0.30024 (2)	0.18362 (3)	0.036
Ru(2)	0.74213 (4)	0.30064 (2)	0.35249 (3)	0.035
Ru(3)	0.87033 (4)	0.42779 (2)	0.30511 (3)	0.035
O(1)	1.0089 (5)	0.1606 (3)	0.2575 (4)	0.088
O(2)	1.0368 (4)	0.3242 (3)	0.0189 (4)	0.076
O(3)	0.6915 (4)	0.2068 (3)	0.0617 (4)	0.082
O(4)	0.6164 (5)	0.1545 (3)	0.3024 (4)	0.083
O(5)	0.6337 (5)	0.3448 (3)	0.5417 (3)	0.080
O(6)	0.9533 (4)	0.2276 (3)	0.4678 (4)	0.087
O(7)	0.9914 (6)	0.4103 (3)	0.5114 (4)	0.095
O(8)	1.0608 (4)	0.5332 (3)	0.2365 (4)	0.084
O(9)	0.7071 (5)	0.5485 (3)	0.3740 (4)	0.084
C(1)	0.9573 (5)	0.2121 (4)	0.2328 (5)	0.056
C(2)	0.9729 (5)	0.3170 (3)	0.0806 (5)	0.050
C(3)	0.7585 (5)	0.2407 (3)	0.1071 (4)	0.050
C(4)	0.6630 (6)	0.2092 (4)	0.3239 (5)	0.055
C(5)	0.6727 (6)	0.3288 (3)	0.4693 (4)	0.051
C(6)	0.8776 (6)	0.2567 (3)	0.4209 (4)	0.054
C(7)	0.9445 (6)	0.4143 (3)	0.4355 (5)	0.059
C(8)	0.9864 (5)	0.4953 (3)	0.2592 (5)	0.052
C(9)	0.7698 (6)	0.5034 (3)	0.3486 (4)	0.051
C(11)	0.7006 (4)	0.3766 (2)	0.2311 (3)	0.031
C(12)	0.7709 (4)	0.4026 (3)	0.1643 (4)	0.034
C(13)	0.7434 (4)	0.4518 (3)	0.0722 (4)	0.039
C(14)	0.6772 (7)	0.4042 (4)	-0.0071 (4)	0.066
C(15)	0.6670 (6)	0.5180 (3)	0.0962 (5)	0.056
C(16)	0.8569 (6)	0.4843 (4)	0.0329 (5)	0.060
C(20)	0.4034 (5)	0.4053 (4)	0.1714 (5)	0.059
C(21)	0.4241 (6)	0.4597 (4)	0.2406 (5)	0.065
C(22)	0.3513 (7)	0.4750 (5)	0.3267 (7)	0.096
C(23)	0.2990 (8)	0.4065 (7)	0.3716 (7)	0.103
C(24)	0.3845 (6)	0.3420 (6)	0.3812 (5)	0.082
C(25)	0.3848 (6)	0.2855 (5)	0.3155 (7)	0.080
C(26)	0.3098 (8)	0.2822 (6)	0.2174 (8)	0.100
C(27)	0.2958 (6)	0.3552 (5)	0.1614 (6)	0.075
H(1)	0.96440	0.34700	0.26800	0.04 (1)

[a] $U_{eq} = {}^1/_3\sum_i\sum_j U_{ij}a_i^*a_j^*\mathbf{a}_i\cdot\mathbf{a}_j$.

rotation of the COD ligand. From the crystal structure (see below) we assign the signal at δ 5.35, with the larger ^{195}Pt coupling, to the protons on C(20) and C(21), since

Table II. Selected Bond Lengths (Å) and Bond Angles (deg) for $Ru_3Pt(\mu\text{-}H)\{\mu_4\text{-}\eta^2\text{-}C{\equiv}C(t\text{-}Bu)\}(CO)_9(COD)$ (4)

Bond Lengths			
Pt-Ru(2)	2.645 (1)	Pt-C(11)	1.972 (6)
Pt-C(20)	2.207 (7)	Pt-C(21)	2.229 (8)
Pt-C(24)	2.352 (8)	Pt-C(25)	2.316 (8)
Ru(1)-Ru(2)	2.810 (1)	Ru(1)-Ru(3)	2.815 (1)
Ru(1)-C(1)	1.941 (7)	Ru(1)-C(2)	1.897 (7)
Ru(1)-C(3)	1.911 (6)	Ru(1)-C(11)	2.484 (5)
Ru(1)-C(12)	2.157 (5)	Ru(2)-Ru(3)	2.791 (1)
Ru(2)-C(4)	1.887 (7)	Ru(2)-C(5)	1.891 (7)
Ru(2)-C(6)	1.902 (7)	Ru(2)-C(11)	2.164 (5)
Ru(3)-C(7)	1.925 (7)	Ru(3)-C(8)	1.916 (7)
Ru(3)-C(9)	1.884 (7)	Ru(3)-C(11)	2.291 (5)
Ru(3)-C(12)	2.199 (5)	C-O(carbonyl)	1.138 (9)[a]
C(11)-C(12)	1.332 (7)	C(12)-C(13)	1.545 (8)
C(13)-C(14)	1.527 (9)	C(13)-C(15)	1.511 (9)
C(13)-C(16)	1.536 (9)	C(20)-C(21)	1.363 (11)
C(20)-C(27)	1.505 (10)	C(21)-C(22)	1.503 (12)
C(22)-C(23)	1.506 (15)	C(23)-C(24)	1.502 (15)
C(24)-C(25)	1.348 (13)	C(25)-C(26)	1.532 (14)
C(26)-C(27)	1.512 (14)		

Bond Angles			
Ru(2)-Pt-C(11)	53.5 (2)	Ru(2)-Pt-C(20)	160.2 (2)
Ru(2)-Pt-C(21)	153.2 (2)	Ru(2)-Pt-C(24)	112.1 (3)
Ru(2)-Pt-C(25)	108.7 (3)	Ru(2)-Ru(1)-Ru(3)	59.5 (1)
Ru(2)-Ru(1)-C(11)	47.8 (2)	Ru(2)-Ru(1)-C(12)	78.4 (2)
Ru(1)-Ru(2)-Pt	100.0 (1)	Ru(3)-Ru(2)-Pt	91.1 (1)
Ru(1)-Ru(2)-C(11)	58.2 (2)	Ru(3)-Ru(2)-C(11)	53.3 (2)
Ru(1)-Ru(2)-Ru(3)	60.3 (1)	Ru(1)-Ru(3)-Ru(2)	60.2 (1)
Ru(1)-Ru(3)-C(12)	49.1 (2)	Ru(1)-Ru(3)-C(11)	57.1 (2)
Pt-C(11)-C(12)	150.9 (4)	Ru(2)-C(11)-C(12)	129.3 (4)
C(11)-C(12)-C(13)	131.1 (5)	Ru-C-O	176.8 (6)[a]

[a] Mean value.

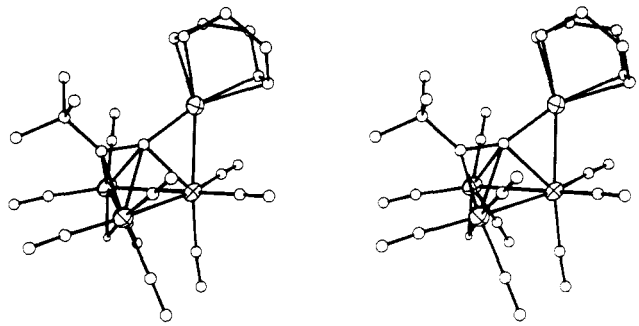

Figure 2. Stereoview of complex **4**.

the Pt–C distances associated with this olefinic bond, endo to the cluster, are significantly shorter.

A $^{13}C\{^1H\}$ NMR spectrum of **4** at 220 K showed that the molecule possessed an effective mirror plane in solution. Five signals were seen in the carbonyl region in the ratio 1:2:2:2:2. Two signals at δ 205.8 (relative intensity 1) and 195.4 (relative intensity 2) broadened considerably on warming to 233 K, and these resonances are assigned to the carbonyls C(6) and C(4)/C(5), respectively, in the unique $Ru(CO)_3$ group on Ru(2) (see below), which are undergoing a tripodal rotation. The other three sharp signals at δ 197.7, 190.4, and 189.4 (relative intensities 2:2:2) are assigned to the equivalent pairs of CO's in the remaining two $Ru(CO)_3$ groups. The signal at δ 190.4 showed a coupling of 13 Hz to the hydride ligand in a ^{1}H-coupled spectrum and is thus assigned to carbonyls C(3)/C(9) which are trans to this ligand. At ambient temperature only one very broad signal at ca. δ 195 is observed in the CO region, indicating complete carbonyl scrambling. The signals at δ 209.4 (J(Pt–C) = 1621 Hz) and 121.9 (J(Pt–C) = 224 Hz) can be assigned respectively, and unambiguously, to the C_α and C_β carbons of the alkynyl ligand, on the basis of their ^{195}Pt couplings. On the same basis, the

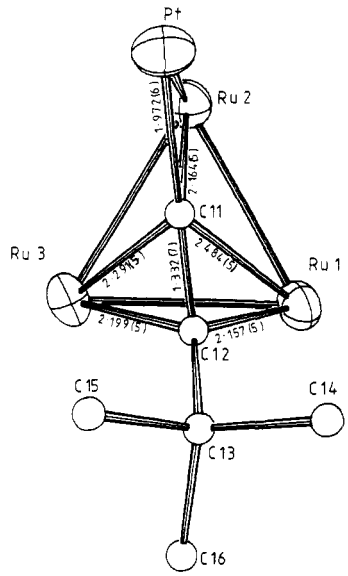

Figure 3. The alkynyl coordination in complex **4**, viewed normal to the Ru_3 plane.

two olefinic resonances at δ 105.2 (J(Pt–C) = 60 Hz) and 92.4 (J(Pt–C) = 134 Hz) are assigned to the carbon pairs C(24)/C(25) and C(20)/C(21), respectively. The rotation of the COD ligand, which was observed in the ^1H spectrum, is also evident in the ^{13}C spectrum, since at ambient temperature a broad resonance at δ 29.6 was observed for the two inequivalent pairs of CH_2 groups, while at 220 K two signals at δ 30.3 and 29.0 were visible.

Molecular Structure of $Ru_3Pt(\mu\text{-}H)\{\mu_4\text{-}\eta^2\text{-}C{\equiv}C(t\text{-}Bu)\}(CO)_9(COD)$ (4). The coordination mode of the alkynyl moiety in **4** was determined by a single-crystal X-ray structure. Figure 1 shows the molecular structure and atomic labeling scheme, while atomic coordinates and important metrical parameters are given in Tables I and II, respectively. A stereoview of the complex is given in Figure 2. The metal core in **4** consists of an essentially equilateral Ru_3 triangle (Ru–Ru distances range from 2.791 (1) to 2.815 (1) Å), with a Pt atom bonded just to Ru(2) (Ru(2)–Pt = 2.645 (1) Å). This results in an overall "out-of-plane" spiked triangular[13] metal core. The angle between the Pt–Ru(2) vector and the normal to the Ru_3 triangle is 10.9°, so the Pt atom can be considered as occupying a pseudoaxial site with respect to Ru(2). Ru–Pt distances in previously reported clusters vary from 2.707 (2) to 2.729 (2) Å in $RuPt_2(\mu\text{-}CO)_3(CO)_2(PPh_2Me)_3$,[14] from 2.721 (1) to 2.741 (1) Å in $RuPt_2(\mu\text{-}CO)_3(CO)_2(PPh_3)_3$,[15] from 2.803 (1) to 2.820 (1) Å in $Ru_2Pt_2(\mu\text{-}H)(\mu_4\text{-}CH)(\mu\text{-}CO)(CO)_2(P\text{-}i\text{-}Pr_3)_2(\eta\text{-}C_5H_5)_2$,[16] and from 2.707 (1) to 2.858 (1) Å in $Ru_2Pt_2(\mu\text{-}H)_2(\mu_4\text{-}C)(\mu\text{-}CO)_2(P\text{-}i\text{-}Pr_3)_2(\eta\text{-}C_5H_5)_2$.[16] The Ru–Pt distance in **4** is somewhat shorter, though comparisons are complicated by the varying ligands which bridge these bonds. Assuming the μ_4-η^2-alkynyl ligand acts as a five-electron donor, complex **4** has 62 cluster valence electrons (CVE's). The Pt atom acts as a 16-electron (pseudo square-planar) center, and so the CVE count is 2 less than the 64 normally associated[13,17] with such a metal framework geometry. This apparent anomalous low CVE count is commonly seen in clusters containing Pt atoms,[17,18] and the metal core found in the 62-electron cluster $Os_3Pt(\mu\text{-}H)_2(\mu_4\text{-}C)(CO)_{10}(PCy_3)$,[19] for example, closely resembles that in **4**.

The idealized coordination mode of the alkynyl in **4** could be described as μ_4-$\eta^2(\perp)$ and as such resembles that found in **3**[12] and the cluster $Fe_2Ni_2(\mu\text{-}PPh_2)(\mu_4\text{-}\eta^2\text{-}C{\equiv}CPh)(CO)_5(\eta\text{-}C_5H_5)_2$ (**5**).[20] In this latter complex the angle between the C≡C axis and the bridged Ni(2)–Fe(2) vector is 90.5°,[21] and the $\perp$ designation is accurate. In complex **4**, however, the angle between the C≡C axis and the bridged Ru(1)—Ru(3) vector is 98.5°, so there is a significant twist away from strict $\perp$ geometry. The details of the alkynyl ligand coordination are illustrated in Figure 3, where the view is normal to the Ru_3 triangle. This twist results in a noticeably longer Ru(1)–C(11) distance of 2.484 (5) Å, as compared with the Ru(3)–C(11) separation of 2.291 (5) Å. The difference between the distances Ru(1)–C(12) = 2.157 (5) Å and Ru(3)–C(12) = 2.199 (5) Å is much less significant. A similar twist is observed in the related complex **3**, and we have suggested[12] that this compound could alternatively be viewed as containing a platinaallenyl ligand coordinated to an Os_3 core.

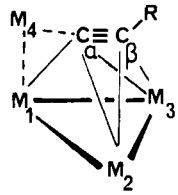

Table III gives relevant structural parameters comparing the M_4–μ_4-$\eta^2(\perp)$-alkynyl bonding mode found in the spiked triangular clusters **3–10** and the closely related M_3–μ_3-$\eta^2(\perp)$ mode[1a-e] observed in cluster complexes where the alkynyl moiety bridges a metal–metal bond. The Δ_α values (i.e. $|D(M(2)\text{–}C_\alpha) - D(M(3)\text{–}C_\alpha)|$) for the μ_3 complexes cover a range of 0.007–0.08 Å, with a mean of 0.026 Å, while the Δ_β values show a similar variation, from 0.0 to 0.072 Å (mean 0.028 Å). These values imply little deviation from strict $\perp$ geometry for most of the μ_3 clusters.

The μ_4-alkynyl complexes, however, show a much greater variation in the Δ_α and Δ_β parameters. For the heterometallic clusters **7–10** (Table III) reported by Vahrenkamp and co-workers,[22,23] where the metal atoms vary considerably in size, it is more meaningful to compare the angle between the C≡C axis and the bridged M—M vector (69, 80, 87, and 73°, respectively, for **7–10**). These latter complexes have been described by the authors as having either $\parallel$[22] or $\perp$[23] bonded alkynyl units, though they are probably

(13) Sappa, E.; Tiripicchio, A.; Carty, A. J.; Toogood, G. E. *Prog. Inorg. Chem.* **1987**, *35*, 437.
(14) Modinos, A.; Woodward, P. *J. Chem. Soc., Dalton Trans.* **1975**, 1534.
(15) Bruce, M. I.; Matisons, J. G.; Skelton, B. W.; White, A. H. *Aust. J. Chem.* **1982**, *35*, 687.
(16) Davies, D. L.; Jeffery, J. C.; Miguel, D.; Sherwood, P.; Stone, F. G. A. *J. Chem. Soc., Chem. Commun.* **1987**, 454.
(17) For a recent overview of electron counting rules in clusters see: Owen, S. M. *Polyhedron* **1988**, *7*, 253.
(18) (a) Mingos, D. M. P.; Wardle, R. W. M. *Transition Met. Chem. (Weinheim, Ger.)* **1985**, *10*, 441. (b) Evans, D. G.; Mingos, D. M. P. *J. Organomet. Chem.* **1982**, *240*, 321.
(19) Farrugia, L. J.; Miles, A. D.; Stone, F. G. A. *J. Chem. Soc., Dalton Trans.* **1985**, 2437.
(20) Weatherell, C.; Taylor, N. J.; Carty, A. J.; Sappa, E.; Tiripicchio, A. *J. Organomet. Chem.* **1985**, *291*, C9.
(21) Calculated from coordinates obtained from the Cambridge Crystallographic Data Base.
(22) Roland, E.; Bernhardt, W.; Vahrenkamp, H. *Chem. Ber.* **1986**, *119*, 2566.
(23) Bernhardt, W.; Vahrenkamp, H. *J. Organomet. Chem.* **1988**, *355*, 427.
(24) Yasufuku, K.; Aoki, K.; Yamazaki, H. *Bull. Chem. Soc. Jpn.* **1975**, *48*, 1616.
(25) Green, M.; Marsden, K.; Salter, I. D.; Stone, F. G. A.; Woodward, P. *J. Chem. Soc., Chem. Commun.* **1983**, 446.
(26) Marinetti, A.; Sappa, E.; Tiripicchio, A.; Tiripicchio Camellini, M. *J. Organomet. Chem.* **1980**, *197*, 335.
(27) Barner-Thorsen, C.; Hardcastle, K. I.; Rosenberg, E.; Siegel, J.; Manotti Landfredi, A. M.; Tiripicchio, A.; Tiripicchio Camellini, M. *Inorg. Chem.* **1981**, *20*, 4306.
(28) Carty, A. J.; MacLaughlin, S. A.; Taylor, N. J.; Sappa, E. *Inorg. Chem.* **1981**, *20*, 4437.

Table III. Structural Parameters in μ_3- and $\mu_4(\perp)$-Alkynyl Complexes

complex	dist, Å: M(1)–C_α / C_α–C_β	M(2)–C_α[a] / M(3)–C_α	M(2)–C_β / M(3)–C_β	Δ_α[b] / Δ_β[c]	M(1)–C_α–C_β / C_α–C_β–R, deg	ref
		μ_4-$\eta^2(\perp)$				
$Os_3Pt(\mu\text{-H})(CCPh)(CO)_{10}(PCy_3)$ (**3**)	2.15 (1)	2.40 (1)	2.23 (1)	0.19	124.4 (8)	12
	1.34 (1)	2.59 (1)	2.15 (1)	0.08	128.6 (9)	
$Fe_2Ni_2(\mu\text{-}PPh_2)(CCPh)(CO)_5(Cp)_2$ (**5**)	1.923 (6)[d]	2.051 (5)	1.969 (6)	0.022	141.7	20
	1.313 (8)	2.073 (6)	2.007 (6)	0.038	136.6	
$Ru_3Pt(\mu\text{-H})(CC(t\text{-Bu}))(CO)_9(COD)$ (**4**)	2.164 (5)	2.291 (5)	2.199 (5)	0.193	129.3 (4)	this work
	1.332 (7)	2.484 (5)	2.157 (5)	0.042	131.1 (5)	
$Ru_3Pt(\mu\text{-H})(CC(t\text{-Bu}))(CO)_9(dppe)$ (**6**)	2.202 (6)	2.396 (6)	2.213 (6)	0.031	129.4 (5)	this work
	1.332 (8)	2.427 (6)	2.209 (6)	0.004	135.2 (6)	
$Co_2FeRu(CCPh)(CO)_{10}(Cp)$ (**7**)	1.90 (1)[e]	2.07 (1)	2.12 (1)	0.53	126.1 (9)	22
	1.37 (2)	2.60 (1)	2.10 (1)	0.02	129 (1)	
$Co_2RuW(CCPh)(CO)_{11}(Cp)$ (**8**)	1.91 (1)[f]	2.26 (1)	2.29 (1)	0.13	137.2 (7)	22
	1.30 (1)	2.39 (1)	2.13 (1)	0.16	135 (1)	
$Co_2NiRu(CCMe)(CO)_8(PPh_3)(Cp)$ (**9**)	1.907 (8)[e]	2.177 (8)	2.049 (9)	0.067	140.7	23
	1.33 (1)	2.244 (8)	2.206 (9)	0.157	141.4	
$CoMo_2Ru(CCMe)(CO)_9(Cp)_2$ (**10**)	1.916 (4)[g]	2.279 (4)	2.323 (4)	0.265	129.5	23
	1.335 (6)	2.544 (4)	2.126 (5)	0.197	132.1	
		μ_3-$\eta^2(\perp)$				
$Fe_3(CCPh)(CO)_7(Cp)$	1.829 (6)	2.006 (5)	2.031 (5)	0.034	152.9 (4)	24
	1.299 (9)	2.040 (4)	2.081 (5)	0.05	144.7 (5)	
$[Fe_3\{CCOC(O)Me\}(CO)_9]^-$	1.809 (6)	2.033 (5)	2.047 (5)	0.011	150.6 (4)	2u
	1.314 (8)	2.044 (5)	2.011 (5)	0.036	143.4 (5)	
$Fe_2W(CCPh)(CO)_8(Cp)$	1.999 (15)[h]	2.011 (10)	2.086 (12)	0.014	163	25
	1.30 (2)	2.025 (11)	2.091 (13)	0.005	141	
$Fe_2Ni(CC(t\text{-Bu}))(CO)_6(Cp)$	1.813 (10)[d]	1.929 (10)	2.034 (10)	0.08	155.8 (9)	26
	1.284 (14)	2.010 (10)	2.060 (10)	0.03	142.8 (9)	
$Ru_3(\mu\text{-H})(CC(t\text{-Bu}))(CO)_9$	1.947 (3)	2.207 (3)	2.268 (3)	0.007	153.7 (2)	9
	1.315 (3)	2.214 (3)	2.271 (3)	0.003	141.0 (2)	
$Ru_3(CC(t\text{-Bu}))(CO)_9]^-$	1.95 (2)	2.16 (2)	2.24 (2)	0.02	156 (1)	27
	1.27 (3)	2.18 (2)	2.24 (2)	0.0	141 (2)	
$Ru_3(\mu\text{-H})(CC(t\text{-Bu}))(CO)_8(PPh_2OEt)$	1.946 (4)	2.194 (4)	2.252 (4)	0.015	154.5 (1)	28
	1.320 (6)	2.209 (4)	2.243 (4)	0.009	140.2 (2)	
$Ru_3(\mu\text{-H})(CC(t\text{-Bu}))(CO)_7(C_6H_{10})$	1.944 (21)	2.165 (13)	2.243 (20)	0.04	156.6 (14)	29
	1.303 (27)	2.209 (13)	2.252 (14)	0.01	141.8 (16)	
$Ru_3(\mu\text{-H})\{CCC(Ph)=CH_2\}(CO)_9$	1.904 (14)	2.178 (15)	2.188 (14)	0.01	156 (1)	30
	1.272 (22)	2.190 (15)	2.276 (14)	0.09	146 (1)	
$Ru_3(\mu\text{-H})(CC(t\text{-Bu}))(CO)_7(dppm)$	1.964 (9)	2.197 (7)	2.309 (7)	0.018	na	31
	1.285 (12)	2.215 (10)	2.286 (1)	0.023	na	
$Hg[Ru_3(CC(t\text{-Bu}))(CO)_9]_2$[i]	1.97 (3)	2.15 (3)	2.24 (4)	0.03	156 (3)	32
	1.30 (4)	2.18 (3)	2.28 (3)	0.04	143 (3)	
$[Ru_3(\mu\text{-HgBr})(CC(t\text{-Bu}))(CO)_9]_2$	1.96 (2)	2.19 (2)	2.25 (2)	0.01	154 (2)	33
	1.31 (3)	2.20 (2)	2.26 (2)	0.01	140 (2)	
$Ru_3(\mu\text{-}AuPPh_3)(CC(t\text{-Bu}))(CO)_9$	1.95 (1)	2.19 (1)	2.27 (1)	0.03	152 (1)	34
	1.29 (2)	2.22 (1)	2.21 (1)	0.06	139 (1)	
$Ru_3(\mu\text{-}CuPPh_3)(CC(t\text{-Bu}))(CO)_9$	1.945 (7)	2.203 (6)	2.260 (7)	0.008	154.4 (5)	35
	1.313 (9)	2.211 (7)	2.259 (6)	0.001	139.9 (7)	
$Ru_3(\mu\text{-}PPh_2)(CC(t\text{-Bu}))(CO)_8$	2.046 (4)	2.242 (4)	2.470 (4)	0.073	157.9 (1)	5
	1.242 (5)	2.315 (4)	2.398 (4)	0.072	154.3 (2)	
$Os_3(\mu\text{-H})(CCCF_3)(CO)_9$	1.937 (10)	2.262 (10)	2.179 (10)	0.009	147.5 (2)	8
	1.33 (1)	2.271 (10)	2.181 (9)	0.003	133.9 (9)	

[a] M(2) is arbitrarily chosen as metal with shortest M–C_α distance. [b] $\Delta_\alpha = |D(M(2)\text{–}C_\alpha - D(M(3)\text{–}C_\alpha)|$. [c] $\Delta_\beta = |D(M(2)\text{–}C_\beta) - D(M(3)\text{–}C_\beta)]$. [d] M(1), M(3) = Fe; M(2) = Ni. [e] M(1), M(2) = Co; M(3) = Ru. [f] M(1) = Co; M(2) = W; M(3) = Ru. [g] M(1) = Co; M(2) = Mo; M(3) = Ru. [h] M(1) = W; M(2), M(3) = Fe. [i] Average values are quoted for two independent molecules.

best regarded as having intermediate geometries. The available structural data suggest that the μ_4-η^2-bonding mode in spiked triangular clusters is a very flexible one, and a wide spectrum of alkynyl–cluster interactions are possible. In addition to a low-energy twist deformation of the alkynyl unit relative to the metal triangle, it is likely that the potential energy surface for the motion of the exo metal relative to the triangle is a soft one. For instance in the closely related group of complexes **7**–**10**[22,23] the angle between the exo metal–metal bond and the normal to the triangle varies from 24.8° for **7** to 10.1° for **9**. The observed solid-state configurations may well be determined by crystal packing forces. The ^{13}C NMR data for **4**, which imply a time-averaged C_s structure even at low temperatures, suggest that the twist deformation observed in the solid state may not persist in solution.

The Ru–C_α distances in **4** (and **6**) are greater than the corresponding separations found in the μ_3 complexes, while the Ru–C_β distances are rather similar. The C_α atom is tipped up toward the M(4) center in the μ_4 systems, with the result that complex **4** has a relatively short Pt–C(11)

(29) Aime, S.; Milone, L.; Sappa, E.; Tiripicchio, A.; Tiripicchio Camellini, M. *Inorg. Chim. Acta* **1979**, *32*, 163.
(30) Ermer, S.; Karpelus, R.; Miura, S.; Rosenberg, E.; Tiripicchio, A.; Landfredi, A. *J. Organomet. Chem.* **1980**, *187*, 81.
(31) Predieri, G.; Tiripicchio, A.; Vignali, C.; Sappa, E. *J. Organomet. Chem.* **1988**, *342*, C33.
(32) Ermer, S.; King, K.; Hardcastle, K. I.; Rosenberg, E.; Manotti Landfredi, A. M.; Tiripicchio, A.; Tiripicchio Camellini, M. *Inorg. Chem.* **1983**, *22*, 1339.
(33) Fahmy, R.; King, K.; Rosenberg, E.; Tiripicchio, A.; Tiripicchio Camellini, M. *J. Am. Chem. Soc.* **1980**, *102*, 3626.
(34) Braunstein, P.; Predieri, G.; Tiripicchio, A.; Sappa, E. *Inorg. Chim. Acta* **1982**, *63*, 113.
(35) Brice, R. A.; Pearse, S. C.; Salter, I. D.; Henrick, K. *J. Chem. Soc., Dalton Trans.* **1986**, 2181.

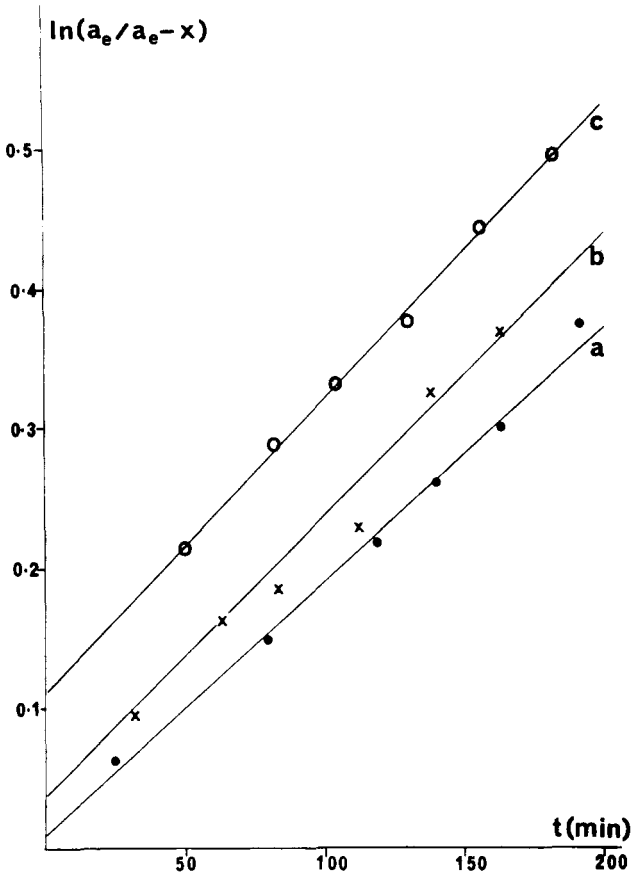

Figure 4. Kinetic plot of the conversion of **6** to **11** in CD_2Cl_2 at 296 K: (a) pure **6**; (b) **6** in presence of NEt_3 (1:1.1 molar ratio); (c) **6** in presence of pyridine (1:2.75 molar ratio). The rate constants k are as follows: for (a) 1.8 (±0.2) and for (b) and (c) 2.1 (±0.2) × 10^{-3} min^{-1}. For clarity the plot for (c) is displaced by 0.1 unit along the ordinate.

distance of 1.972 (6) Å. In the complexes $Ni_2M_2\{\mu_4$-η^4-C=C(H)C(Me)=$CH_2\}(CO)_6(\eta$-$C_5H_5)_2$ (M = Fe,[36] Ru[37]), which also contain an "out-of-plane" spiked triangular metal core coordinated to an alkyne-derived fragment, the degree of interaction between the C_α atom and the spiked metal (M = Fe, M–C_α = 2.266 (8) Å;[36] M = Ru, M–C_α = 2.46 (3) Å[37]) is considerably weaker. The C_α–C_β distances (Table III) in the μ_4 complexes (mean = 1.33, range 1.30 (1)–1.37 (2) Å) are slightly greater than those observed in the μ_3 complexes (mean 1.296, range 1.242 (5)–1.33 (1) Å), while the bend-back angles M(1)–C_α–C_β and C_α–C_β–R are more acute in the μ_4 case. This is consistent with a rehybridization of the carbon atoms in the μ_4-alkynyl unit toward greater sp^2 character. Such trends have been previously noted by Carty and co-workers.[5,38]

The COD ligand is asymmetrically bonded to the Pt atom, the exo Pt–C(olefin) distances (2.316 (8) and 2.352 (8) Å) being greater than the Pt–C(olefin) distances endo to the cluster (2.207 (7) and 2.229 (8) Å). This may be ascribed to the differing trans effects of the Pt–Ru and Pt–C bonds. The directly located hydride ligand bridges the Ru(1)–Ru(3) bond, this position being consistent with that determined by using potential energy minimization calculations (HYDEX[39]). The hydride-bridged Ru–Ru

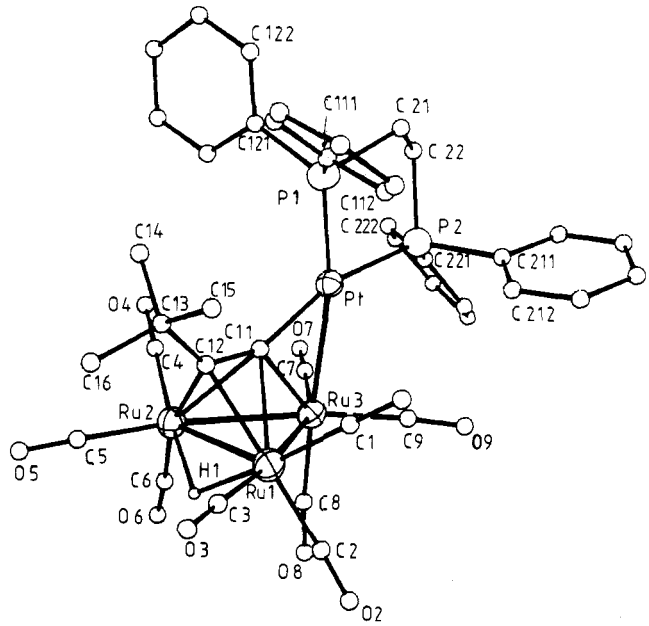

Figure 5. Molecular structure of the complex $Ru_3Pt(\mu$-H$)\{\mu_4$-η^2-C≡C(t-Bu)$\}(CO)_9$(dppe) (**6**).

vector (2.815 (1) Å) is only marginally longer than the other two Ru–Ru distances (2.810 (1) and 2.791 (1) Å). In complex **2a** the hydride-bridged Ru–Ru vector (2.792 (3) Å) is also similar in magnitude to the unbridged bonds (2.795 (3) and 2.799 (3) Å), and this is attributed[9] to an exact balance between the bond lengthening effect of a hydride ligand[40] and the shortening effect of the alkynyl moiety.

Reactivity of Complex 4. In spite of the relatively short Pt–Ru distance observed in the crystal structure of **4**, the Pt–Ru bond appears to be weak and is easily cleaved. Thus on treatment of **4** with CO the precursor triruthenium cluster **2a** is rapidly regenerated, together with an insoluble brown-purple material. This material appears to be a polymeric Pt carbonyl $[Pt_x(CO)_y]_n$ on the basis of IR and analytical evidence. Furthermore, reaction of **4** with $Os_3(\mu$-H$)_2(CO)_{10}$ affords, via transfer of the Pt(COD) unit, the tetrahedral triosmium–platinum cluster $Os_3Pt(\mu$-H$)_2(\mu$-CO$)(CO)_9$(COD)[41] and complex **2a**. However, on treatment of **4** with bis(diphenylphosphino)ethane (dppe) the COD ligand is displaced, leaving the Ru_3Pt core intact. Two complexes are formed and have been identified by spectroscopic and crystallographic techniques as the orange hydrido alkynyl complex $Ru_3Pt(\mu$-H$)\{\mu_4$-η^2-C≡C(t-Bu)$\}$-$(CO)_9$(dppe) (**6**) and the tautomeric red vinylidene cluster $Ru_3Pt(\mu_4$-η^2-C=C(H)t-Bu$)(CO)_9$(dppe) (**11**).

Complexes **6** and **11** can be separated by chromatography on a Florosil column and recrystallized below 0 °C, but crystalline samples of **6** are often contaminated with small amounts of **11**. ^{1}H NMR studies show that **6** is the initial product and that is readily isomerizes at ambient temperatures to **11**. This process appears to be accelerated by the chromatography. Solutions of pure samples of **11** soon show NMR signals due to **6**, thus demonstrating that the tautomerization is reversible. The rate of conversion of **6** to **11** at 296 K was followed, and good first-order kinetics were observed (Figure 4).

$$6 \underset{k_{-1}}{\overset{k_1}{\rightleftharpoons}} 11$$

A first-order rate constant, k (i.e. $k_1 + k_{-1}$), of 1.8 (±0.2)

(36) Marchino, M. L. N.; Sappa, E.; Manotti Landfredi, A. M.; Tiripicchio, A. *J. Chem. Soc., Dalton Trans.* **1984**, 1541.
(37) Lanfranchi, M.; Tiripicchio, A.; Tiripicchio Camellini, M.; Gambino, O.; Sappa, E. *Inorg. Chim. Acta* **1982**, *64*, L269.
(38) MacLaughlin, S. A.; Taylor, N. J.; Carty, A. J. *Organometallics* **1982**, *2*, 1194.
(39) Orpen, A. G. *J. Chem. Soc., Dalton Trans.* **1980**, 2509.
(40) Teller, R. G.; Bau, R. *Struct. Bonding (Berlin)* **1981**, *44*, 1.
(41) Ewing, P.; Farrugia, L. J. *J. Organomet. Chem.* **1988**, *347*, C31.

Table IV. Final Positional Parameters (Fractional Coordinates) with Esd's in Parentheses and Isotropic Thermal Parameters (Equivalent Isotropic Parameters U_{eq} for Anisotropic Atoms) for $Ru_3Pt(\mu\text{-}H)\{\mu_4\text{-}\eta^2\text{-}C{\equiv}C(t\text{-}Bu)\}(CO)_9(dppe)$ (6)[a]

	x/a	y/b	z/c	U_{eq}, Å^2
Pt	−0.03658 (2)	0.23885 (1)	0.64743 (1)	0.030
Ru(1)	0.12946 (4)	0.31174 (3)	0.47951 (3)	0.042
Ru(2)	0.15640 (3)	0.15472 (3)	0.49742 (3)	0.035
Ru(3)	−0.02907 (3)	0.21680 (3)	0.49560 (3)	0.036
P(1)	−0.00526 (11)	0.25663 (10)	0.77490 (8)	0.038
P(2)	−0.19613 (10)	0.23554 (10)	0.67911 (8)	0.034
O(1)	0.0380 (5)	0.4424 (4)	0.5634 (4)	0.103
O(2)	0.0390 (5)	0.3625 (4)	0.3261 (4)	0.118
O(3)	0.3223 (4)	0.3877 (3)	0.4568 (3)	0.086
O(4)	0.1020 (4)	0.0312 (3)	0.6067 (3)	0.067
O(5)	0.3643 (3)	0.1062 (3)	0.4830 (4)	0.085
O(6)	0.1001 (4)	0.0563 (3)	0.3592 (3)	0.079
O(7)	−0.1374 (4)	0.0749 (3)	0.5346 (3)	0.068
O(8)	−0.0448 (4)	0.1898 (4)	0.3233 (3)	0.087
O(9)	−0.1999 (4)	0.3229 (4)	0.4793 (3)	0.099
C(1)	0.0735 (6)	0.3934 (4)	0.5319 (4)	0.064
C(2)	0.0697 (5)	0.3428 (5)	0.3831 (5)	0.071
C(3)	0.2515 (6)	0.3591 (4)	0.4662 (4)	0.061
C(4)	0.1233 (5)	0.0781 (4)	0.5654 (4)	0.046
C(5)	0.2882 (5)	0.1271 (4)	0.4904 (4)	0.049
C(6)	0.1177 (5)	0.0928 (4)	0.4105 (4)	0.052
C(7)	−0.0974 (5)	0.1290 (4)	0.5220 (3)	0.046
C(8)	−0.0342 (5)	0.1994 (5)	0.3884 (4)	0.057
C(9)	−0.1363 (5)	0.2839 (5)	0.4888 (4)	0.061
C(11)	0.0817 (4)	0.2389 (3)	0.5872 (3)	0.034
C(12)	0.1769 (4)	0.2463 (3)	0.5825 (3)	0.033
C(13)	0.2608 (4)	0.2621 (4)	0.6394 (4)	0.043
C(14)	0.2519 (5)	0.2082 (4)	0.7056 (4)	0.054
C(15)	0.2496 (5)	0.3427 (4)	0.6670 (4)	0.057
C(16)	0.3603 (4)	0.2523 (5)	0.6074 (4)	0.064
C(21)	−0.1206 (4)	0.2742 (4)	0.8201 (3)	0.044
C(22)	−0.1967 (4)	0.2229 (4)	0.7842 (3)	0.042
C(111)	0.0654 (4)	0.3376 (4)	0.8066 (3)	0.046
C(112)	0.0371 (5)	0.4078 (4)	0.7764 (4)	0.059
C(113)	0.0874 (6)	0.4721 (5)	0.7937 (5)	0.082
C(114)	0.1690 (7)	0.4673 (6)	0.8397 (6)	0.091
C(115)	0.2008 (6)	0.4000 (6)	0.8697 (5)	0.080
C(116)	0.1494 (5)	0.3349 (4)	0.8526 (4)	0.059
C(121)	0.0395 (4)	0.1753 (4)	0.8286 (4)	0.046
C(122)	0.0475 (5)	0.1741 (5)	0.9083 (4)	0.064
C(123)	0.0792 (6)	0.1104 (7)	0.9462 (5)	0.082
C(124)	0.1032 (7)	0.0475 (6)	0.9062 (7)	0.096
C(125)	0.0965 (6)	0.0468 (5)	0.8278 (6)	0.080
C(126)	0.0633 (5)	0.1102 (4)	0.7901 (4)	0.054
C(211)	−0.2580 (4)	0.3259 (4)	0.6686 (3)	0.037
C(212)	−0.2089 (4)	0.3885 (4)	0.6455 (4)	0.049
C(213)	−0.2534 (6)	0.4581 (4)	0.6406 (5)	0.068
C(214)	−0.3500 (5)	0.4645 (4)	0.6580 (4)	0.061
C(215)	−0.3988 (5)	0.4031 (5)	0.6813 (4)	0.058
C(216)	−0.3550 (4)	0.3340 (4)	0.6866 (4)	0.050
C(221)	−0.2825 (4)	0.1665 (4)	0.6420 (3)	0.040
C(222)	−0.2842 (5)	0.0945 (4)	0.6728 (4)	0.059
C(223)	−0.3509 (7)	0.0416 (5)	0.6434 (5)	0.083
C(224)	−0.4113 (5)	0.0596 (5)	0.5841 (5)	0.070
C(225)	−0.4091 (5)	0.1292 (5)	0.5519 (4)	0.065
C(226)	−0.3454 (5)	0.1826 (4)	0.5803 (4)	0.051
H(1)	0.18790	0.23890	0.44020	0.06 (2)

[a] $U_{eq} = {}^1/_3\sum_i\sum_j U_{ij}a_i^*a_j^*\mathbf{a}_i\cdot\mathbf{a}_j$.

× 10^{-3} min^{-1} was obtained. In the presence of added base, either NEt_3 or pyridine, this rate constant was found to be identical within experimental error. The interconversion of **6** and **11** involves a reversible formal migration of a hydrogen atom from a metal–metal edge to the β-carbon of the alkynyl ligand. Since the rate is unaffected by added base, our results clearly preclude, as the primary mechanism, a dissociative route involving a rate-determining protonation or deprotonation, but they are consistent with an intramolecular hydride migration. The vinylidene complex **11** is the thermodynamically favored product, and the equilibrium constant $K = k_1/k_{-1}$ was measured as 12 (±1) at 298 K.

Table V. Selected Bond Lengths (Å) and Bond Angles (deg) for $Ru_3Pt(\mu\text{-}H)\{\mu_4\text{-}\eta^2\text{-}C{\equiv}C(t\text{-}Bu)\}(CO)_9(dppe)$ (6)

Bond Lengths			
Pt–Ru(3)	2.681 (1)	Pt–P(1)	2.267 (2)
Pt–P(2)	2.304 (2)	Pt–C(11)	1.985 (6)
Ru(1)–Ru(2)	2.824 (1)	Ru(1)–Ru(3)	2.792 (1)
Ru(1)–C(1)	1.896 (8)	Ru(1)–C(2)	1.921 (9)
Ru(1)–C(3)	1.913 (8)	Ru(1)–C(11)	2.396 (6)
Ru(1)–C(12)	2.213 (6)	Ru(1)–H(1)	1.686 (1)
Ru(2)–Ru(3)	2.796 (1)	Ru(2)–C(4)	1.872 (7)
Ru(2)–C(5)	1.902 (7)	Ru(2)–C(6)	1.927 (8)
Ru(2)–C(11)	2.427 (6)	Ru(2)–C(12)	2.209 (6)
Ru(2)–H(1)	1.857 (1)	Ru(3)–C(7)	1.890 (8)
Ru(3)–C(8)	1.891 (7)	Ru(3)–C(9)	1.903 (8)
Ru(3)–C(11)	2.202 (6)	C–O(carbonyl)	1.13 (1)[a]
C(11)–C(12)	1.332 (8)	C(12)–C(13)	1.521 (8)
C(13)–C(14)	1.508 (10)	C(13)–C(15)	1.518 (10)
C(13)–C(16)	1.521 (9)	C(21)–C(22)	1.509 (9)
Bond Angles			
Ru(3)–Pt–C(11)	53.8 (2)	Ru(3)–Pt–P(1)	166.7 (1)
Ru(3)–Pt–P(2)	108.2 (1)	P(1)–Pt–P(2)	85.0 (1)
C(11)–Pt–P(1)	113.0 (2)	C(11)–Pt–P(2)	161.9 (2)
Ru(3)–Ru(1)–Ru(2)	59.7 (1)	Ru(3)–Ru(1)–C(11)	49.5 (2)
Ru(3)–Ru(1)–C(12)	79.0 (2)	Ru(3)–Ru(2)–Ru(1)	59.6 (1)
Ru(3)–Ru(2)–C(11)	49.2 (2)	Ru(3)–Ru(2)–C(12)	79.0 (2)
Pt–C(11)–C(12)	151.2 (5)	Ru(3)–C(11)–C(12)	129.4 (5)
C(11)–C(12)–C(13)	135.2 (6)	Ru–C–O	176.8 (8)[a]

[a] Mean value.

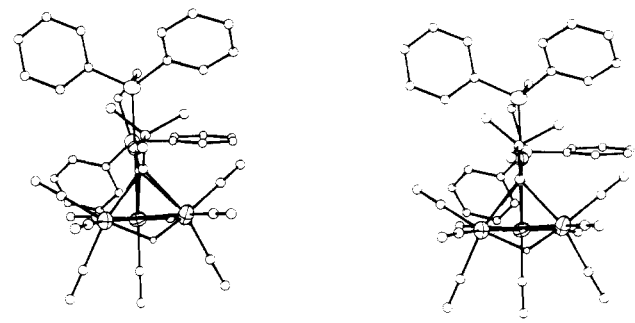

Figure 6. Stereoview of complex **6**.

Molecular Structure of $Ru_3Pt(\mu\text{-}H)\{\mu_4\text{-}\eta^2\text{-}C{\equiv}C(t\text{-}Bu)\}(CO)_9(dppe)$ (6). The molecular structure of **6** is shown in Figure 5, and atomic coordinates and important metrical parameters are given in Tables IV and V, respectively. The overall structure of **6** closely resembles that of **4**, with the COD ligand replaced by a chelating dppe unit. The Pt–P distance associated with the endo P(1) (2.267 (2) Å) is significantly shorter than that of the exo P(2) (2.304 (2) Å), as was seen for the Pt–C distances associated with the chelating COD ligand in **4**. The most significant difference between **6** and **4** lies in the bonding of the μ_4-η^2-alkynyl unit to the spiked triangular Ru_3Pt core. In complex **6** the Ru–C_α distances (Ru(1)–C(11) = 2.396 (6), Ru(2)–C(11) = 2.427 (6) Å) differ only slightly, and the Δ_α value of 0.031 Å is only marginally greater than the mean value of 0.026 Å for those μ_3 structures given in Table III. This results in an angle between the Ru(1)–Ru(2) and C(11)–C(12) vectors of 91.3°, so that the ⊥ designation is more accurate for **6** than for **4**. The Ru_3Pt core in **6** is very similar to that in **4** (see Tables II and V), with an angle of 7.1° between the Ru(3)–Pt vector and the normal to the Ru_3 plane. The disposition of the phenyl groups of the dppe ligand removes the pseudomirror symmetry of the cluster core, as can be seen in the stereoview of complex **6** (Figure 6).

Molecular Structure of $Ru_3Pt(\mu_4\text{-}\eta^2\text{-}C{=}C(H)t\text{-}Bu)(CO)_9(dppe)$ (11). The molecular structure of **11** is

Table VI. Final Positional Parameters (Fractional Coordinates) with Esd's in Parentheses and Isotropic Thermal Parameters (Equivalent Isotropic Parameters U_{eq} for Anisotropic Atoms) for $Ru_3Pt(\mu_4\text{-}\eta^2\text{-}C{=}C(H)t\text{-}Bu)(CO)_9(dppe)\cdot 2C_6H_{12}$ (11)[a]

	x/a	y/b	z/c	U_{eq}, Å^2
Pt	0.12351 (1)	−0.05393 (5)	0.10970 (2)	0.038
Ru(1)	0.13203 (2)	0.08138 (9)	0.21073 (5)	0.043
Ru(2)	0.12637 (2)	−0.13702 (10)	0.22474 (5)	0.042
Ru(3)	0.18358 (2)	−0.02928 (10)	0.31116 (5)	0.044
P(1)	0.11006 (8)	−0.19197 (30)	0.03608 (17)	0.046
P(2)	0.11184 (8)	0.05763 (31)	0.02235 (15)	0.044
O(1)	0.1692 (3)	0.2716 (9)	0.1967 (6)	0.112
O(2)	0.1176 (3)	0.1789 (10)	0.3134 (5)	0.107
O(3)	0.0625 (3)	0.1101 (11)	0.1132 (5)	0.095
O(4)	0.1041 (3)	−0.1004 (10)	0.3246 (5)	0.110
O(5)	0.1480 (3)	−0.3687 (10)	0.2680 (7)	0.122
O(6)	0.0590 (3)	−0.2001 (13)	0.1319 (5)	0.116
O(7)	0.2368 (3)	0.1378 (11)	0.3497 (6)	0.120
O(8)	0.1681 (3)	0.0319 (10)	0.4206 (5)	0.090
O(9)	0.2232 (3)	−0.2154 (10)	0.3996 (5)	0.098
C(1)	0.1542 (4)	0.2023 (12)	0.2003 (7)	0.067
C(2)	0.1235 (5)	0.1427 (13)	0.2767 (7)	0.074
C(3)	0.0886 (4)	0.1007 (14)	0.1447 (7)	0.066
C(4)	0.1141 (4)	−0.1142 (14)	0.2896 (7)	0.074
C(5)	0.1416 (4)	−0.2827 (13)	0.2514 (9)	0.082
C(6)	0.0843 (4)	−0.1742 (15)	0.1636 (7)	0.070
C(7)	0.2165 (3)	0.0778 (14)	0.3377 (7)	0.062
C(8)	0.1722 (3)	0.0078 (13)	0.3783 (8)	0.066
C(9)	0.2083 (3)	−0.1487 (13)	0.3635 (6)	0.057
C(11)	0.1608 (3)	−0.0494 (10)	0.2078 (5)	0.037
C(12)	0.1929 (3)	−0.0524 (10)	0.2232 (5)	0.041
C(13)	0.2131 (3)	−0.1470 (12)	0.2188 (7)	0.056
C(14)	0.2038 (3)	−0.2613 (12)	0.2279 (7)	0.064
C(15)	0.2108 (4)	−0.1381 (13)	0.1514 (7)	0.079
C(16)	0.2485 (3)	−0.1262 (14)	0.2703 (7)	0.078
C(21)	0.1164 (3)	−0.1370 (12)	−0.0305 (6)	0.060
C(22)	0.0997 (3)	−0.0270 (11)	−0.0500 (6)	0.051
C(111)	0.1295 (3)	−0.3233 (11)	0.0596 (8)	0.049 (4)
C(112)	0.1233 (3)	−0.3895 (10)	0.1014 (8)	0.053 (4)
C(113)	0.13899 (16)	−0.48986 (64)	0.12286 (31)	0.078 (5)
C(114)	0.1609 (3)	−0.5241 (11)	0.1025 (8)	0.102 (6)
C(115)	0.1671 (3)	0.4579 (10)	0.0607 (8)	0.101 (6)
C(116)	0.15147 (16)	−0.35748 (64)	0.03929 (31)	0.087 (5)
C(121)	0.0688 (3)	−0.2268 (15)	−0.0046 (5)	0.044 (3)
C(122)	0.0586 (3)	−0.3230 (11)	−0.0416 (8)	0.073 (5)
C(123)	0.0260 (4)	−0.3466 (10)	−0.0770 (6)	0.086 (5)
C(124)	0.0037 (3)	−0.2739 (15)	−0.0755 (5)	0.085 (5)
C(125)	0.0139 (3)	−0.1777 (11)	−0.0385 (8)	0.082 (5)
C(126)	0.0465 (4)	−0.1542 (10)	−0.0031 (6)	0.055 (4)
C(211)	0.0813 (3)	0.1595 (13)	−0.0001 (9)	0.050 (4)
C(212)	0.0495 (4)	0.1360 (10)	−0.0435 (7)	0.067 (4)
C(213)	0.0262 (3)	0.2167 (16)	−0.0587 (5)	0.083 (5)
C(214)	0.0347 (3)	0.3208 (13)	−0.0306 (9)	0.090 (6)
C(215)	0.0666 (4)	0.3443 (10)	0.0128 (7)	0.102 (6)
C(216)	0.0899 (3)	0.2636 (16)	0.0280 (5)	0.073 (5)
C(221)	0.1451 (2)	0.1349 (11)	0.0254 (4)	0.046 (3)
C(222)	0.1399 (3)	0.1999 (14)	−0.0284 (5)	0.065 (4)
C(223)	0.16528 (19)	0.25651 (85)	−0.02890 (43)	0.078 (5)
C(224)	0.1958 (2)	0.2482 (11)	0.0244 (4)	0.067 (4)
C(225)	0.2010 (3)	0.1833 (14	0.0782 (5)	0.070 (4)
C(226)	0.17564 (19)	0.12664 (85)	0.07865 (43)	0.048 (3)
C(301)	0.0853 (10)	0.4525 (38)	0.8538 (18)	0.18 (2)
C(302)	0.0615 (9)	0.3830 (30)	0.8218 (18)	0.14 (1)
C(303)	0.0470 (8)	0.3802 (31)	0.7507 (19)	0.16 (1)
C(304)	0.0520 (11)	0.4673 (41)	0.7180 (20)	0.20 (2)
C(305)	0.0729 (10)	0.5468 (32)	0.7476 (20)	0.17 (1)
C(306)	0.0839 (9)	0.5488 (33)	0.8226 (20)	0.17 (1)
C(401)	0.3178 (8)	0.1233 (29)	0.6258 (17)	0.15 (1)
C(402)	0.2961 (8)	0.0794 (31)	0.6493 (16)	0.15 (1)
C(403)	0.2791 (9)	0.0003 (31)	0.6166 (19)	0.16 (1)
C(404)	0.2575 (8)	0.0307 (29)	0.5508 (18)	0.15 (1)
C(405)	0.2705 (10)	0.0653 (33)	0.5191 (18)	0.18 (1)
C(406)	0.2981 (8)	0.1542 (29)	0.5553 (17)	0.15 (1)
C(501)	1.000	0.050 (5)	0.750	0.12 (2)
C(502)	0.9759 (10)	−0.0232 (35)	0.7608 (19)	0.11 (1)
C(503)	0.9762 (10)	−0.1230 (37)	0.7508 (20)	0.12 (1)
C(504)	1.000	−0.173 (5)	0.750	0.11 (2)
H(12)	0.20457	0.01867	0.23922	0.080

[a] $U_{eq} = {}^1/_3\sum_i\sum_j U_{ij}a_i^*a_j^*\mathbf{a}_i\cdot\mathbf{a}_j$.

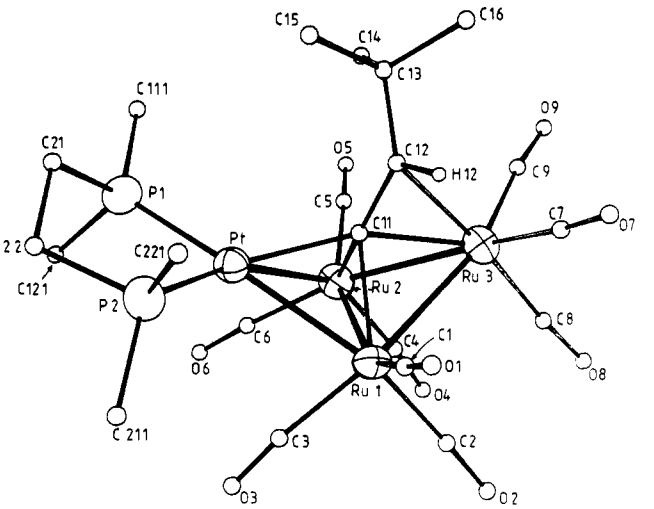

Figure 7. Molecular structure of $Ru_3Pt(\mu_4\text{-}\eta^2\text{-}C{=}C(H)t\text{-}Bu)(CO)_9(dppe)$ (11). Phenyl groups on the dppe ligand are omitted for clarity; contact carbons only are shown.

Table VII. Selected Bond Lengths (Å) and Bond Angles (deg) for $Ru_3Pt(\mu_4\text{-}\eta^2\text{-}C{=}C(H)t\text{-}Bu)(CO)_9(dppe)$ (11)

Bond Lengths			
Pt–Ru(1)	2.730 (1)	Pt–Ru(2)	2.792 (1)
Pt–P(1)	2.260 (4)	Pt–P(2)	2.276 (4)
Pt–C(11)	2.120 (10)	Ru(1)–Ru(2)	2.708 (2)
Ru(1)–Ru(3)	2.799 (2)	Ru(1)–C(1)	1.892 (15)
Ru(1)–C(2)	1.908 (16)	Ru(1)–C(3)	1.916 (15)
Ru(1)–C(11)	2.123 (12)	Ru(2)–Ru(3)	2.823 (2)
Ru(2)–C(4)	1.873 (15)	Ru(2)–C(5)	1.905 (17)
Ru(2)–C(6)	1.880 (15)	Ru(2)–C(11)	2.142 (12)
Ru(3)–C(7)	1.903 (16)	Ru(3)–C(8)	1.927 (16)
Ru(3)–C(9)	1.901 (16)	Ru(3)–C(11)	2.123 (10)
Ru(3)–C(12)	2.297 (11)	C–O(carbonyl)	1.12 (2)[a]
C(11)–C(12)	1.391 (16)	C(12)–C(13)	1.535 (18)
C(13)–C(14)	1.51 (2)	C(13)–C(15)	1.52 (2)
C(13)–C(16)	1.555 (19)		

Bond Angles			
Ru(1)–Pt–Ru(2)	58.7 (1)	Ru(1)–Pt–P(2)	106.0 (1)
Ru(2)–Pt–P(1)	108.6 (1)	P(1)–Pt–P(2)	84.9 (2)
Ru(1)–Pt–C(11)	50.0 (4)	Ru(2)–Pt–C(11)	49.4 (3)
Pt–Ru(1)–Ru(2)	61.8 (1)	Ru(3)–Ru(1)–Pt	97.9 (1)
Pt–Ru(1)–C(11)	49.9 (3)	Ru(3)–Ru(1)–C(11)	48.8 (3)
Pt–Ru(2)–Ru(1)	59.5 (1)	Pt–Ru(2)–Ru(3)	95.9 (1)
Pt–Ru(2)–C(11)	48.7 (3)	Ru(3)–Ru(2)–C(11)	48.3 (3)
Ru(1)–Ru(3)–Ru(2)	57.6 (1)	Ru(1)–Ru(3)–C(11)	48.8 (4)
Ru(2)–Ru(3)–C(11)	48.8 (4)	Ru(1)–Ru(3)–C(12)	77.5 (3)
Ru(2)–Ru(3)–C(12)	80.8 (3)	Pt–C(11)–C(12)	122.3 (8)
Ru(1)–C(11)–C(12)	131.0 (9)	Ru(2)–C(11)–C(12)	141.3 (9)
Ru(3)–C(11)–C(12)	78.6 (7)	C(11)–C(12)–C(13)	130.4 (12)
C(11)–C(12)–H(12)	115.0 (12)	Ru(3)–C(12)–C(11)	65.0 (6)
Ru(3)–C(12)–C(13)	122.7 (9)	Ru(3)–C(12)–H(12)	82.6 (7)
C(13)–C(12)–H(12)	114.7 (11)	Ru–C–O	174 (1)[a]

[a] Mean value.

shown in Figure 7, and atomic coordinates and important metrical parameters are given in Tables VI and VII, respectively. The transformation of **6** to **11** results in a modification of the cluster core from the spiked triangular arrangement found in **6** to a butterfly geometry in **11**. The Pt atom occupies one wingtip of the butterfly, and the vinylidene ligand bridges across the open face such that the C_α atom C(11) is bonded to all four metal atoms, and the C=C bond is formally π-bonded to the wingtip Ru atom. This μ_4-vinylidene coordination mode has been previously observed in the clusters $M_3Ni(\mu\text{-}H)(\mu_4\text{-}\eta^2\text{-}C{=}C(H)R)(CO)_9(\eta\text{-}C_5H_5)$ (M = Ru, R = *t*-Bu (**12**),[42] R = *i*-Pr

(42) (a) Sappa, E.; Tiripicchio, A.; Tiripicchio Camellini, M. *J. Chem. Soc., Chem. Commun.* **1979**, 254. (b) Sappa, E.; Tiripicchio, A.; Tiripicchio Camellini, M. *Inorg. Chim. Acta* **1980**, *41*, 11. In these papers the complex is erroneously formulated, see ref 43.

(**13**)[43]; M = Os, R = *t*-Bu (**14**)[44]), $Co_3Fe(\mu_4\text{-}\eta^2\text{-}C{=}CH_2)(\mu\text{-}CO)_2(CO)_7(\eta\text{-}C_5H_5)$ (**15**),[45] and $Ru_4(\mu\text{-}PPh_2)(\mu\text{-}OH)(\mu_4\text{-}\eta^2\text{-}C{=}C(H)i\text{-}Pr)(CO)_{10}$ (**16**).[46] The dihedral butterfly angle in **11** (117.8 (1)°) is similar in value to those found in the closely related complexes **12** (116.6°),[42] **13** (118.3°),[43] and **14** (117.1°)[44] but smaller than found in **15** (124°)[45] or **16** (143.7°).[46] The hinge vector Ru(1)–Ru(2) = 2.708 (1) Å is significantly shorter than the wingtip–hinge Ru–Ru distances of 2.799 (1) and 2.823 (2) Å. These latter distances differ significantly (12σ) from each other as do the two Pt–Ru separations (60σ difference), which are somewhat longer than those observed in **4** and **6**. These internal discrepancies may be due to the asymmetry introduced by the bulky *t*-Bu group.

The C_α atom C(11) is approximately equidistant from the four metal centers (M–C(11) = 2.120 (10)–2.142 (12) Å), and the wingtip Ru–C_β separation (Ru(3)–C(12) = 2.297 (11) Å) compares well with the corresponding distances found in **12** (2.227 (10) Å),[42] **13** (2.219 (6) Å),[43] **14** (2.25 (2) Å),[44] and **15** (2.267 (5) Å).[45] Consistent with a decrease in formal bond order, the C_α—C_β distance in **11** (C(11)–C(12) = 1.391 (16) Å) is slightly longer than the corresponding distances in **6** and related alkynyl complexes (Table III), though it is marginally shorter than the C=C separations observed in other μ_4 vinylidene clusters.[42-46]

The Hydrido Alkynyl–Vinylidene Rearrangement. The transition-metal-mediated conversion of a terminal alkyne (coordinated or otherwise) to a vinylidene ligand provides a useful synthetic route to mono- or polynuclear transition-metal vinylidene complexes.[47,48] This reaction, which involves a formal 1,2-hydrogen shift, is often thought[47a,48a,b] to proceed via an initial oxidative addition of the C–H bond of the alkyne giving a hydrido alkynyl complex, which then further rearranges to the vinylidene compound. In a theoretical study on the alkyne–vinylidene interconversion, Silvestre and Hoffmann[49] conclude that the isomerization via a hydrido alkynyl intermediate, in mononuclear complexes at least, was of much higher energy than one involving an η^1-alkyne slippage and consequent 1,2-hydrogen shift. In bi- and trinuclear clusters, however, the conversion of a hydrido alkynyl to vinylidene was considered much more likely.[49] To our knowledge however, in only a few examples reported by Werner and co-workers[50] have isolable hydrido alkynyl complexes been shown to undergo thermal rearrangement to vinylidene compounds, and these reactions involve *mononuclear* Rh and Ir species. In the cluster context there are numerous known examples of stable hydrido alkynyl species such as $M_3(\mu\text{-}H)(\mu_3\text{-}\eta^2\text{-}C{\equiv}CR)(CO)_9$ (M = Os;[8,51] M = Ru[30,43,52]), $Os_3(\mu\text{-}H)(\mu_2\text{-}\eta^2\text{-}C{\equiv}CPh)(CO)_9(L)$ (L = CO, PMe_2Ph[51a,53]), and $Re_2(\mu\text{-}H)(\mu_2\text{-}\eta^2\text{-}C{\equiv}CPh)(CO)_8$,[54] which demonstrate no tendency to convert to vinylidene species. These observations may readily be understood in terms of simple electron counting rules: in cluster compounds the $\mu_{3,4}\text{-}\eta^2$-alkynyl unit acts as a formal five-electron donor, while the $\mu_2\text{-}\eta^2$ unit acts as formal three-electron donor; however the $\mu_{3,4}\text{-}\eta^2$-vinylidene is a four-electron donor, while the $\mu_2\text{-}\eta^2$ ligand is a two-electron donor. The $\mu_{3,4} \rightarrow \mu_{3,4}$ (or $\mu_2 \rightarrow \mu_2$) hydrido alkynyl to vinylidene transformation therefore involves a formal loss of two electrons donated by the ligands. In order to obey accepted electron counting rules,[17] the stoichiometric rearrangement requires the formation of a new metal–metal bond, either by a core rearrangement (as seen here) or through cluster unsaturation. Alternatively the rearrangement process could be promoted by the addition of a two-electron donor ligand, though there is little evidence that this is the case.[55]

The tautomerization exhibited by complexes **6** and **11** represents the first example, to our knowledge, of a reversible transformation of a hydrido alkynyl to vinylidene

Scheme I

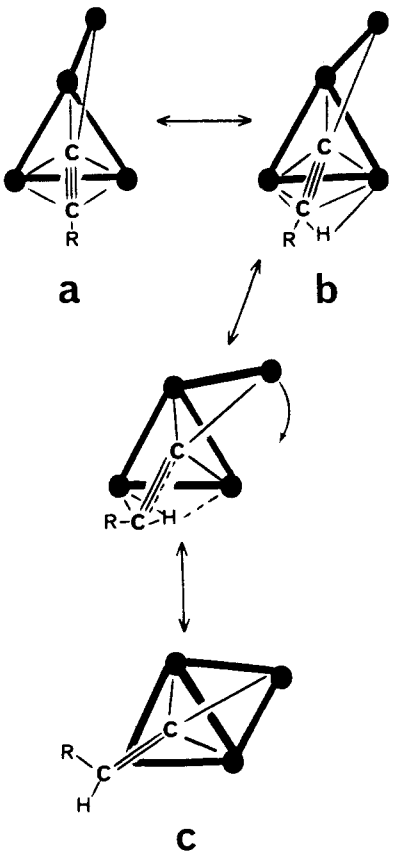

(43) Carty, A. J.; Taylor, N. J.; Sappa, E.; Tiripicchio, A. *Inorg. Chem.* **1983**, *22*, 1871.
(44) Sappa, E.; Tiripicchio, A.; Tiripicchio Camellini, M. *J. Organomet. Chem.* **1983**, *246*, 287.
(45) Brun, P.; Dawkins, G. M.; Green, M.; Mills, R. M.; Salaün, J.-Y.; Stone, F. G. A.; Woodward, P. *J. Chem. Soc., Dalton Trans.* **1983**, 1357.
(46) Carty, A. J.; MacLaughlin, S. A.; Taylor, N. J. *J. Chem. Soc., Chem. Commun.* **1981**, 476.
(47) (a) Bruce, M. I.; Swincer, A. G. *Adv. Organomet. Chem.* **1983**, *22*, 59. (b) Bruce, M. I. *Pure Appl. Chem.* **1986**, *58*, 553.
(48) For recent examples see: (a) Al-Obaidi, Y. N.; Green, M.; White, N. D.; Taylor, G. E. *J. Chem. Soc., Dalton Trans.* **1982**, 319. (b) Bernhardt, W.; Vahrenkamp, H. *Angew. Chem., Int. Ed. Engl.* **1984**, *23*, 141. (c) v. Schnering, C.; Albiez, T.; Bernhardt, W.; Vahrenkamp, H. *Ibid.* **1986**, *25*, 479. (d) Roland, E.; Bernhardt, W.; Vahrenkamp, H. *Chem. Ber.* **1985**, *118*, 2858. (e) Albiez, T.; Bernhardt, W.; v. Schnering, C.; Roland, E.; Vahrenkamp, H. *Ibid.* **1987**, *120*, 141. (f) Adams, J. S.; Bitcon, C.; Brown, J. R.; Collison, D.; Cuningham, M.; Whitely, M. W. *J. Chem. Soc., Dalton Trans.* **1987**, 3049. (g) Berry, D. H.; Eisenberg, R. *J. Am. Chem. Soc.* **1985**, *107*, 7181. (h) Pourreau, D. B.; Geoffroy, G. L.; Rheingold, A. L.; Geib, S. J. *Organometallics* **1986**, *5*, 1337.
(49) Silvestre, J.; Hoffmann, R. *Helv. Chim. Acta* **1985**, *68*, 1461.
(50) (a) Garcia Alonso, F. J.; Höhn, A.; Wolf, J.; Otto, H.; Werner, H. *Angew. Chem., Int. Ed. Engl.* **1985**, *24*, 406. (b) Höhn, A.; Otto, H.; Dziallas, M.; Werner, H. *J. Chem. Soc., Chem. Commun.* **1987**, 852. (c) Werner, H.; Wolf, J.; Garcia Alonso, F. J.; Ziegler, M. L.; Serhadli, O. *J. Organomet. Chem.* **1987**, *336*, 397.
(51) (a) Deeming, A. J.; Hasso, S.; Underhill, M. *J. Chem. Soc., Dalton Trans.* **1975**, 1614. (b) Sappa, E.; Tiripicchio, A.; Landfredi, A. *J. Organomet. Chem.* **1983**, *249*, 391. (c) Gambino, O.; Ferrari, R. P.; Chinone, M.; Vaglio, G. A. *Inorg. Chim. Acta* **1975**, *12*, 155. (d) Aime, S.; Milone, L.; Deeming, A. J. *J. Chem. Soc., Chem. Commun.* **1980**, 1168.
(52) Sappa, E.; Gambino, O.; Milone, L.; Cetini, G. *J. Organomet. Chem.* **1972**, *39*, 169.
(53) Koridze, A. A.; Kizas, O. A.; Petrovskii, P. V.; Kolobova, N. E.; Struchkov, Yu. T.; Yanovsky, A. I. *J. Organomet. Chem.* **1988**, *338*, 81.
(54) Nubel, P. O.; Brown, T. L. *Organometallics* **1984**, *3*, 29.
(55) Complexes of the type $M_3(\mu\text{-}H)(\mu_3\text{-}\eta^2\text{-}CCR)(CO)_9$ are stable to CO, and treatment with tertiary phosphines results in simple carbonyl substitution, see, for example: Jangala, C.; Rosenberg, E.; Skinner, D.; Aime, S.; Milone, L.; Sappa, E. *Inorg. Chem.* **1980**, *19*, 1571.

ligand in a cluster complex. We believe this tautomerization is facilitated by a soft potential energy surface for the deformation of the Ru_3Pt core. Scheme I shows the proposed metal core/ligand transformation leading from complex **6** (geometry **a**) via the twisted geometry **b** (modeled by the solid-state structure of **4**) to the vinylidene complex **11** (geometry **c**).[56] The kinetic data outlined above support an intramolecular mechanism. Vahrenkamp et al.[22,23] have also suggested that facile metal core rearrangements occur in their related M_4-μ_4-η^2-alkynyl systems. While the migration of hydrides from metal–metal edges to C atoms (forming new C–H bonds, presumably via agostic M(μ-H)C interactions) is commonly seen in cluster reactions,[2,57] only rarely are reversible processes reported.[58] Interestingly Shapley and co-workers[59] have recently shown such migrations can also occur as degenerate, i.e. fluxional, processes in hydrido triosmium clusters.

Finally, in the context of the cluster–surface analogy,[4] it is interesting to note that multisite bound vinylidene ligands have often been postulated, on both mechanistic[60] and theoretical[61] grounds, as intermediates in the formation of alkylidyne species from alkenes and alkynes adsorbed at metal surfaces. Although the experimental evidence for vinylidene intermediates in this process is not conclusive,[62] Weinberg and co-workers[63] have recently detected such species from the decomposition of ethylidyne adsorbed on the Ru(001) p(2×2)O surface. Although in this case the EELS data suggest a μ_3-η^2-bonding mode similar to that observed[64] in $Os_3(\mu\text{-H})_2(\mu_3\text{-}\eta^2\text{-C}{=}CH_2)(CO)_9$, the $M_4(\mu_4\text{-}\eta^2)$ coordination mode seen in **11** may represent a possibility for vinylidene binding at stepped metal surfaces. In addition, the metal framework rearrangement, which accompanies the ligand transformation in complexes **6** and **11**, may also provide a molecular model for the restructuring of metal surfaces during heterogeneous catalytic reactions.[65]

Spectroscopic Data and Fluxional Behavior of Complexes 6 and 11. Solution NMR data are consistent with the crystal structures. The ^1H spectra of **6** and **11** show the expected resonances for the *t*-Bu and dppe groups, and for **6** a singlet at δ −19.12 is observed due to the Ru(μ-H)Ru proton. At 233 K the $^{31}P\{^1H\}$ spectrum of

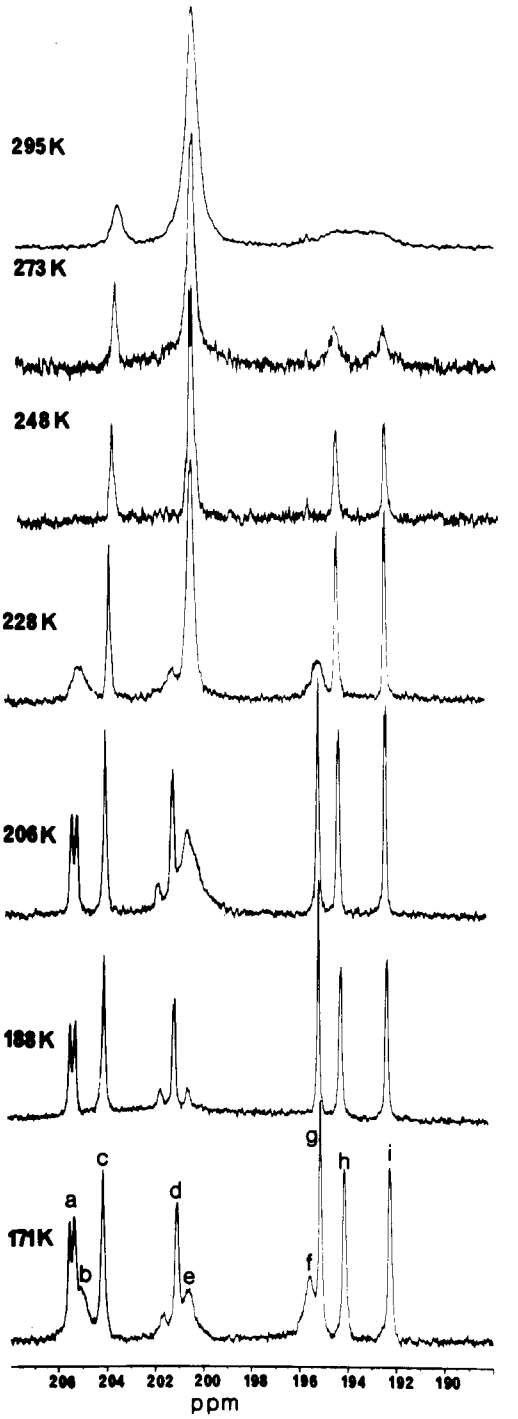

Figure 8. Variable-temperature $^{13}C\{^1H\}$ NMR spectrum of complex **11** in the carbonyl region.

complex **6** shows two narrow ($\Delta\nu_{1/2} \sim 1$ Hz) doublets at δ 46.5 (J(Pt–P) = 4152 Hz) and 51.8 (J(Pt–P) = 2643 Hz), indicative of inequivalent P environments. These resonances may be assigned[66] to P(1) and P(2), respectively. The signals show broadening at 295 K ($\Delta\nu_{1/2} \sim 10$ Hz), and at this temperature weak *but sharp* resonances due to small amounts of **11** can be observed. These results clearly indicate that the line broadening is due to an *intramolecular* exchange of the two inequivalent P environments of the chelating dppe ligand in **6** rather than due to the slow chemical exchange between **6** and **11**. The Pt(dppe) fragment is presumably rotating, in a process similar to that observed for the COD ligand in **4**. From a line-shape analysis we estimate $\Delta G^*_{295} = 63.2$ (5) kJ mol^{-1} for this exchange.

(56) The transition state may involve a μ_4-acetylide bridging a butterfly framework, see: Lanfranchi, M.; Tiripicchio, A.; Sappa, E.; MacLaughlin, S. A.; Carty, A. J. *J. Chem. Soc., Chem. Commun.* **1982**, 538.
(57) For a recent example see: Skinner, D. M.; Rosenberg, E.; Bracker-Novak, J.; Aime, S.; Osella, D.; Gobetto, R.; Milone, L. *Organometallics* **1988**, *7*, 856.
(58) (a) Calvert, R. B.; Shapley, J. R. *J. Am. Chem. Soc.* **1978**, *100*, 7726. (b) Cree-Uchiyama, M.; Shapley, J. R.; St. George, G. M. *Ibid.* **1986**, *108*, 1316.
(59) (a) VanderVelde, D. G.; Holmgren, J. S.; Shapley, J. R. *Inorg. Chem.* **1987**, *26*, 3077. (b) Kneuper, H.-J.; Shapley, J. R. *Organometallics* **1987**, *6*, 2455.
(60) (a) Kesmodel, L. L.; Dubois, L. H.; Somorjai, G. A. *J. Chem. Phys.* **1979**, *70*, 2180. (b) Megiris, C. E.; Berlowitz, P.; Butt, J. B.; Kung, H. H. *Surf. Sci.* **1985**, *159*, 184.
(61) (a) Minot, C.; Van Hove, M. A.; Somorjai, G. A. *Surf. Sci.* **1982**, *127*, 441. (b) Silvestre, J.; Hoffmann, R. *Langmuir* **1985**, *1*, 621 and references therein.
(62) Avery, N. R. *Langmuir* **1988**, *4*, 445 and references therein.
(63) (a) Hills, M. M.; Parmeter, J. E.; Weinberg, W. H. *J. Am. Chem. Soc.* **1987**, *109*, 597. (b) *Ibid.* **1987**, *109*, 4225.
(64) Deeming, A. J.; Underhill, M. *J. Chem. Soc., Dalton Trans.* **1974**, 1415.
(65) Somorjai, G. A. *Surf. Sci.* **1979**, *89*, 496.
(66) Within similar complexes there is generally a good correlation between shorter Pt–P distances and greater magnitudes of ^1J(Pt–P), see: (a) Verkade, J. G.; Mosbo, J. A. In *Methods in Stereochemical Analysis*; Verkade, J. G., Quin, L. D., Eds.; VCH: Weinheim, 1987; Vol. 8, Chapter 13, pp 425–463. (b) Pregosin, P. S.; Kunz, R. W. In *NMR Basic Principles and Progress*; Diehl, P., Fluck, E., Kosfeld, R., Eds.; Springer-Verlag: New York, 1979; Vol. 16. (c) Hitchcock, P.; Jacobson, B.; Pidcock, A. *J. Chem. Soc., Dalton Trans.* **1977**, 2038, 2043.

At 233 K the ^{13}C spectrum of **6** in the carbonyl region is similar to **4**, with five resonances in the ratio 1:2:2:2:2. This implies an effective molecular mirror plane, and the conformation of the Pt(dppe) unit must therefore be "flipping" rapidly. The signals at δ 207.7 (relative intensity 1) and 195.3 (relative intensity 2), which are assigned to the carbonyls C(8) and C(7)/C(9), respectively, remain sharp on warming to 263 K, while the other three resonances at δ 198.5, 192.4, and 189.9 (each of relative intensity 2) broaden considerably. This indicates that the lowest energy exchange in **6** involves a tripodal rotation of the two equivalent $Ru(CO)_3$ groups, which contrasts with the situation in **4**, where it is the unique $Ru(CO)_3$ group which has the lower barrier to rotation. Signals for the alkynyl C_α and C_β carbons were observed at δ 228.3 (J(P–C) = 15, 75 Hz) and 123.7 (J(P–C) = 5, J(Pt–C) = 178 Hz), respectively. The expected large ^{195}Pt coupling could not be observed for the former resonance, presumably due to the multiplicity of the signal and poor S/N. The chemical shifts of the alkynyl C_α and C_β carbons of complexes **6** and **4** fall in the range of ^{13}C data recently compiled by Carty et al.[67]

At 243 K complex **11** shows an AB pattern in the $^{31}P\{^1H\}$ spectrum, and this signal remains well resolved up to 348 K, precluding any significant exchange of the P environments. The vinylidene C=C(*H*) proton appears at δ 5.75 as a pseudotriplet (J(P–H) = 4.5, 5.0 Hz) in the ^1H spectrum, due to similar couplings to the inequivalent ^{31}P nuclei. In accord with the lack of a symmetry element in **11**, the ^{13}C NMR spectrum at the lowest temperature measured 171 K showed nine CO resonances (Figure 8). Three signals b, e, and f at ca. δ 205.2, 200.6, and 195.6, respectively are broad and evidently exchanging at this temperature. On warming to 188 K these collapse into the base line and on further raising of the temperature coalesce to a broad signal at ca. δ 200.4 at the mean chemical shift. At the fast-exchange regime (248 K) an *averaged* ^{31}P coupling of 5.5 Hz is visible. Above 206 K resonances a, d, and g at δ 205.4, 201.1, and 195.1 begin to broaden and coalesce at 273 K to an *averaged* signal fortuitously also at δ 200.5, the mean of their chemical shifts. At 273 K resonances c, h, and i also broaden, with h and i broadening faster than c. The b/e/f and a/d/g exchanges are assigned to independent tripodal rotations of two $Ru(CO)_3$ groups, and from line-shape analysis we obtain $\Delta G^\ddagger$ = 43 (1) and 48 (1) kJ mol^{-1}, respectively for these processes. The broadening of resonances c, h, and i is not solely due to a tripodal rotation of an $Ru(CO)_3$ group, and other processes such as inter-Ru–CO exchange must also be occurring.

Complex **11** posseses a pseudo mirror plane, disturbed principally by the differing substituents on the vinylidene ligand. It is reasonable to suppose that the ^{31}P couplings for CO ligands related by this pseudo mirror plane are similar. On the basis of the fluxional behavior and by comparison with the ^{31}P couplings observed in complex **17** (see below), we assign the resonances b, e, and f to one of the hinge $Ru(CO)_3$ groups and resonances a, d, and g to the other hinge $Ru(CO)_3$ moiety. The *mean* ^{31}P coupling in the latter group of resonances is 4.9 Hz, which is close to the *averaged* value of 5.5 Hz observed for the b/e/f signal at fast exchange at 248 K. Of the remaining resonances both h and i have a small ^{31}P coupling, and we assign these to the C(7)/C(9) pair, with c being assigned to C(8). Since the b/e/f tripodal rotation is of lower energy than that of the a/d/g group, we tentatively assign these

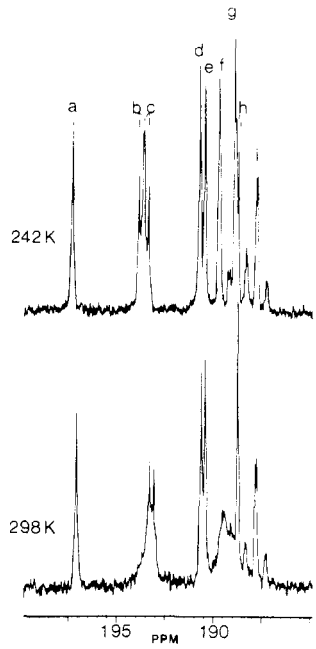

Figure 9. Variable-temperature $^{13}C\{^1H\}$ NMR spectrum of complex **17** in the carbonyl region.

former signals to the CO's on Ru(1), on the basis of steric arguments. The $Ru(CO)_3$ group on Ru(1) is proximate to H(12), and the barrier to tripodal rotation may be expected to be smaller than that of the $Ru(CO)_3$ group on Ru(2), which is proximate to the bulky *t*-Bu group.

Protonation of Complexes 6 and 11. The alkynyl to vinylidene ligand isomerization involves a formal reduction in the CC bond order. The reactivity of **11** toward dihydrogen was investigated in the hope of inducing further reduction to alkylidyne species, but no tractable products were isolated. However, complex **11** is readily protonated by $HBF_4{\cdot}Et_2O$ to give high yields of the hydrido vinylidene cationic cluster $[Ru_3Pt(\mu\text{-}H)(\mu_4\text{-}\eta^2\text{-}C{=}C(H)t\text{-}Bu)(CO)_9(dppe)]^+BF_4^-$ (**17**). The presence of a hydride bridging an Ru–Ru edge was indicated by a low frequency resonance at δ –20.34 (J(Pt–H) = 13 Hz) in the ^1H NMR spectrum. Other signals in the ^1H, ^{13}C, and ^{31}P NMR spectra were very similar to those of **11** (see Experimental Section), implying little structural rearrangement has taken place. The NMR data do not allow unambiguous placement of the hydride ligand, though by analogy with complexes **12**–**14**[42-44] we suspected the hinge Ru–Ru vector as the site of protonation. This was confirmed by a single-crystal X-ray study (see below, Figure 10).

The variable-temperature ^{13}C NMR spectra of **17** (Figure 9) show that the presence of the hydride has raised the barriers to the carbonyl exchanges seen in **11**, so that at 298 K six signals are reasonably sharp ($\Delta\nu_{1/2} \sim 5$ Hz), while three are exchange broadened. Couplings to the hydride allow more definitive assignments to be made. Thus resonances d and f (J(H–C) = 13.2, 15.1 Hz, respectively) can be attributed to the carbonyl carbons C(1)/C(5) (Figure 10) trans to the hydride, while resonances b, c, h, and i (with J(H–C) = 3.0–4.0 Hz) are assigned to the four CO's cis to this ligand. Resonances a, e, and g show no coupling to the hydride and are thus assigned to the $Ru(CO)_3$ group on Ru(3). These latter signals show the same ^{31}P coupling pattern observed for complex **11**, with two resonances e and g [C(7)/C(9)] having a ca. 2 Hz coupling, and a [C(8)] having no detectable coupling. Since resonances b, f, and h are broad at 298 K these are presumably due to the $Ru(CO)_3$ group on Ru(1), applying the steric

(67) Carty, A. J.; Cherkas, A. A.; Randall, L. H. *Polyhedron* **1988**, *7*, 1045.

Table VIII. Final Positional Parameters (Fractional Coordinates) with Esd's in Parentheses and Isotropic Thermal Parameters (Equivalent Isotropic Parameters U_{eq} for Anisotropic Atoms) for $[Ru_3Pt(\mu\text{-}H)(\mu_4\text{-}\eta^2\text{-}C{=}C(H)t\text{-}Bu)(CO)_9(dppe)]^+BF_4^-$ (17)[a]

	x/a	y/b	z/c	U_{eq}, Å^2
Pt	0.86414 (3)	0.23767 (2)	0.25959 (2)	0.032
Ru(1)	0.98509 (5)	0.07541 (4)	0.24844 (3)	0.036
Ru(2)	0.79242 (6)	0.09807 (4)	0.11428 (3)	0.037
Ru(3)	0.74911 (6)	−0.05436 (4)	0.21215 (4)	0.041
B	0.4505 (14)	0.3520 (8)	0.7475 (7)	0.075
F(1)	0.4726 (7)	0.2725 (4)	0.7020 (5)	0.123
F(2)	0.3610 (7)	0.3325 (5)	0.8048 (5)	0.131
F(3)	0.4347 (11)	0.4146 (6)	0.6995 (5)	0.183
F(4)	0.5669 (11)	0.3924 (9)	0.7968 (6)	0.229
P(1)	0.79403 (18)	0.36982 (12)	0.21934 (11)	0.040
P(2)	0.94655 (17)	0.33657 (11)	0.38617 (11)	0.036
C(1)	1.0288 (8)	0.0550 (6)	0.3643 (5)	0.060
C(2)	1.0758 (8)	−0.0265 (5)	0.2061 (5)	0.055
C(3)	1.1336 (7)	0.1749 (5)	0.2508 (5)	0.056
C(4)	0.7947 (8)	−0.0036 (6)	0.0215 (5)	0.055
C(5)	0.6151 (9)	0.1096 (6)	0.0734 (5)	0.057
C(6)	0.8631 (9)	0.1973 (5)	0.0504 (5)	0.060
C(7)	0.7759 (9)	−0.1216 (5)	0.3083 (6)	0.065
C(8)	0.8175 (8)	−0.1470 (5)	0.1355 (6)	0.061
C(9)	0.5725 (9)	−0.1187 (5)	0.1712 (5)	0.058
C(11)	0.7790 (6)	0.0936 (4)	0.2481 (4)	0.033
C(12)	0.6898 (7)	0.0638 (4)	0.3065 (5)	0.046
C(13)	0.5476 (8)	0.0748 (5)	0.3196 (5)	0.060
C(14)	0.4619 (8)	0.0831 (6)	0.2352 (7)	0.073
C(15)	0.5518 (8)	0.1686 (6)	0.3796 (6)	0.071
C(16)	0.4817 (9)	−0.0066 (7)	0.3621 (6)	0.074
C(21)	0.7715 (7)	0.4430 (4)	0.3205 (4)	0.044
C(22)	0.9013 (7)	0.4533 (4)	0.3778 (4)	0.045
C(111)	0.6460 (7)	0.3612 (7)	0.1464 (5)	0.049 (2)
C(112)	0.5201 (7)	0.3383 (5)	0.1744 (3)	0.061 (2)
C(113)	0.4056 (4)	0.3318 (4)	0.1170 (4)	0.078 (3)
C(114)	0.4169 (6)	0.3483 (6)	0.0315 (4)	0.077 (3)
C(115)	0.5429 (6)	0.3712 (4)	0.0036 (3)	0.078 (3)
C(116)	0.6574 (5)	0.3776 (5)	0.0610 (4)	0.068 (2)
C(121)	0.9210 (6)	0.4479 (4)	0.1762 (3)	0.045 (2)
C(122)	0.8991 (6)	0.5404 (5)	0.1687 (6)	0.070 (2)
C(123)	0.9997 (7)	0.6061 (4)	0.1445 (6)	0.081 (3)
C(124)	1.1223 (5)	0.5794 (3)	0.1278 (2)	0.078 (3)
C(125)	1.1442 (6)	0.4869 (4)	0.1353 (6)	0.072 (2)
C(126)	1.0435 (7)	0.4212 (4)	0.1595 (6)	0.055 (2)
C(211)	1.1257 (5)	0.3584 (6)	0.4166 (5)	0.040 (2)
C(212)	1.1830 (4)	0.3213 (3)	0.4861 (2)	0.059 (2)
C(213)	1.3215 (5)	0.3363 (5)	0.5050 (4)	0.079 (3)
C(214)	1.4026 (5)	0.3885 (5)	0.4542 (4)	0.075 (3)
C(215)	1.3453 (4)	0.4255 (3)	0.3847 (3)	0.067 (2)
C(216)	1.2068 (5)	0.4105 (6)	0.3658 (5)	0.056 (2)
C(221)	0.8678 (6)	0.2992 (4)	0.4789 (3)	0.041 (2)
C(222)	0.8860 (8)	0.2115 (3)	0.5033 (6)	0.063 (2)
C(223)	0.8293 (7)	0.1816 (4)	0.5755 (5)	0.086 (3)
C(224)	0.7545 (5)	0.2395 (3)	0.6234 (2)	0.071 (2)
C(225)	0.7363 (8)	0.3272 (3)	0.5990 (5)	0.065 (2)
C(226)	0.7930 (6)	0.3571 (4)	0.5268 (5)	0.052 (2)
O(1)	1.0639 (8)	0.0402 (5)	0.4310 (4)	0.098
O(2)	1.1315 (7)	−0.0853 (4)	0.1834 (5)	0.085
O(3)	1.2248 (6)	0.2315 (4)	0.2503 (5)	0.089
O(4)	0.8020 (7)	−0.0598 (4)	−0.0358 (4)	0.082
O(5)	0.5129 (6)	0.1140 (5)	0.0426 (4)	0.081
O(6)	0.9068 (8)	0.2507 (4)	0.0101 (4)	0.096
O(7)	0.7950 (8)	−0.1556 (5)	0.3673 (5)	0.113
O(8)	0.8547 (7)	−0.2040 (4)	0.0914 (4)	0.085
O(9)	0.4648 (6)	−0.1570 (4)	0.1442 (4)	0.080
H(1)	0.96430	0.09420	0.14660	0.080
H(12)	0.74590	0.06430	0.37640	0.080

[a] $U_{eq} = {}^1/_3\sum_i\sum_i U_{ij}a_i^*a_j^*\mathbf{a}_i\cdot\mathbf{a}_j$.

arguments outlined above. The signals c, d, and i may therefore be assigned to the CO's on Ru(2).

The molecular structure of complex **17** is shown in Figure 10, and atomic coordinates and important metrical parameters are given in Tables VIII and IX, respectively. As expected from the spectroscopic data, the overall configuration of **17** is very similar to that of **11**. The presence of a hydrido ligand bridging the Ru(1)–Ru(2) bond in **17** is indicated by a lengthening of this vector by ca. 0.13 Å over that observed in **11**. Residual electron density was observed at this position, and potential energy minimization calculations[39] also indicated a "hole" of suitably low energy. Apart from the usual increase in the bend-back Ru–C–O angles associated with the CO groups cis to the hydride, other differences between **11** and **17** are marginal. The butterfly angle of 117.8 (1)° is identical with that found in **11** and suggests that this parameter is principally

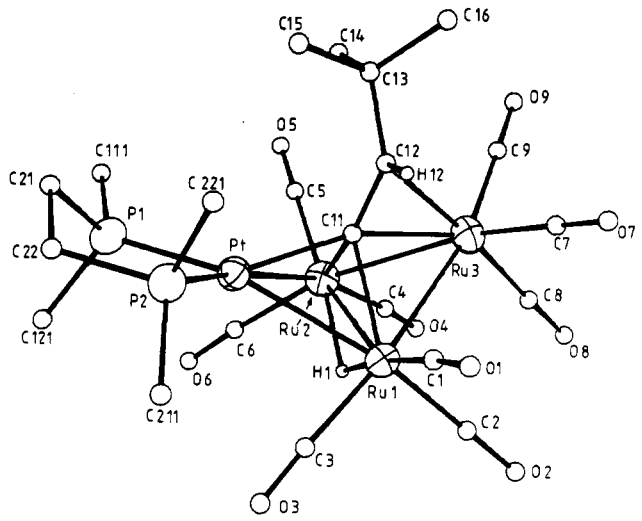

Figure 10. Molecular structure of the cation $[Ru_3Pt(\mu\text{-}H)(\mu_4\text{-}\eta^2\text{-}C{=}C(H)t\text{-}Bu)(CO)_9(dppe)]^+$ (**17**). Phenyl groups on the dppe ligand are omitted for clarity; contact carbons only are shown.

Table IX. Selected Bond Lengths (Å) and Bond Angles (deg) for $[Ru_3Pt(\mu\text{-}H)(\mu_4\text{-}\eta^2\text{-}C{=}C(H)t\text{-}Bu)(CO)_9(dppe)]^+BF_4^-$ (17)

Bond Lengths			
Pt–Ru(1)	2.784 (1)	Pt–Ru(2)	2.782 (1)
Pt–P(1)	2.269 (2)	Pt–P(2)	2.286 (2)
Pt–C(11)	2.092 (6)	Ru(1)–Ru(2)	2.835 (1)
Ru(1)–Ru(3)	2.774 (1)	Ru(1)–C(1)	1.896 (9)
Ru(1)–C(2)	1.917 (8)	Ru(1)–C(3)	1.910 (8)
Ru(1)–C(11)	2.155 (7)	Ru(1)–H(1)	1.648 (1)
Ru(2)–Ru(3)	2.830 (1)	Ru(2)–C(4)	1.915 (8)
Ru(2)–C(5)	1.904 (9)	Ru(2)–C(6)	1.928 (8)
Ru(2)–C(11)	2.112 (7)	Ru(2)–H(1)	1.793 (1)
Ru(3)–C(7)	1.911 (9)	Ru(3)–C(8)	1.915 (9)
Ru(3)–C(9)	1.909 (9)	Ru(3)–C(11)	2.089 (6)
Ru(3)–C(12)	2.278 (7)	B–F(1)	1.320 (13)
B–F(2)	1.354 (15)	B–F(3)	1.262 (14)
B–F(4)	1.361 (17)	C–O(carbonyl)	1.13 (1)[a]
C(11)–C(12)	1.400 (10)	C(12)–C(13)	1.508 (11)
C(13)–C(14)	1.547 (13)	C(13)–C(15)	1.525 (12)
C(13)–C(16)	1.515 (13)		
Bond Angles			
Ru(1)–Pt–Ru(2)	61.2 (1)	Ru(1)–Pt–P(2)	109.4 (1)
Ru(2)–Pt–P(1)	104.8 (1)	P(1)–Pt–P(2)	84.1 (1)
Ru(1)–Pt–C(11)	50.0 (2)	Ru(2)–Pt–C(11)	48.9 (2)
Pt–Ru(1)–Ru(2)	59.3 (1)	Ru(3)–Ru(1)–Pt	95.6 (1)
Pt–Ru(1)–C(11)	48.0 (2)	Ru(3)–Ru(1)–C(11)	48.2 (2)
Pt–Ru(2)–Ru(1)	59.4 (1)	Pt–Ru(2)–Ru(3)	94.4 (1)
Pt–Ru(2)–C(11)	48.2 (2)	Ru(3)–Ru(2)–C(11)	47.3 (2)
Ru(1)–Ru(3)–Ru(2)	60.8 (1)	Ru(1)–Ru(3)–C(11)	50.2 (2)
Ru(2)–Ru(3)–C(11)	48.0 (2)	Ru(1)–Ru(3)–C(12)	77.9 (2)
Ru(2)–Ru(3)–C(12)	80.6 (2)	Pt–C(11)–C(12)	119.9 (5)
Ru(1)–C(11)–C(12)	127.0 (5)	Ru(2)–C(11)–C(12)	142.0 (5)
Ru(3)–C(11)–C(12)	78.8 (4)	C(11)–C(12)–C(13)	134.4 (7)
C(11)–C(12)–H(12)	111.5 (6)	Ru(3)–C(12)–C(11)	64.1 (4)
Ru(3)–C(12)–C(13)	124.3 (5)	Ru(3)–C(12)–H(12)	108.6 (5)
C(13)–C(12)–H(12)	106.9 (6)	Ru–C–O	176.3 (8)[a]

[a] Mean value.

Table X. Experimental Data for Crystallographic Studies

	4	6	11	17
compd formula	$C_{23}H_{22}O_9PtRu_3$	$C_{41}H_{34}O_{92}PtRu_3$	$C_{41}H_{34}O_9P_2PtRu_3 \cdot 2C_6H_{12}$	$C_{41}H_{35}BF_4O_9P_2PtRu_3$
M_r	940.72	1230.96	1378.1	1318.8
space group	$P2_1/n$ (No. 14, C_{2h}^5)	$P2_1/n$	$C2/c$ (No. 15, C_{2h}^6)	$P\bar{1}$ (No. 2, C_i^1)
cryst system	monoclinic	monoclinic	monoclinic	triclinic
a/Å	11.283 (3)	13.867 (3)	47.561 (5)	10.189 (4)
b/Å	17.843 (2)	17.725 (2)	12.176 (2)	14.329 (4)
c/Å	13.625 (3)	17.429 (7)	23.155 (10)	15.596 (9)
α/deg				97.70 (4)
β/deg	94.06 (2)	92.50 (2)	118.27 (2)	94.72 (4)
γ/deg				98.75 (3)
V/Å^3	2736 (1)	4280 (2)	11 810 (6)	2218 (2)
Z	4	4	8	2
D_{calcd}/g cm^{-3}	2.28	1.91	1.55	1.97
$F(000)$	1768	2368	5336	1268
μ(Mo Kα)/cm^{-1}	67.9	44.3	32.2	43.0
θ range/deg	$2 < \theta < 25$	$2 < \theta < 25$	$2 < \theta < 25$	$2 < \theta < 25$
cryst size/mm	0.3 × 0.3 × 0.2	0.2 × 0.3 × 0.4	0.29 × 0.43 × 0.35	0.33 × 0.4 × 0.5
range of trans coeff corr	0.86/1.20	0.76/1.36	0.73/1.31	0.85/1.33
no. of data collected	5259	8122	11 065	8253
no. of unique data	4813	7508	10 382	7786
std reflctns	$\bar{5}53$, $\bar{1}8\bar{5}$, $2\bar{9}4$	$6\bar{3}0$, $2\bar{5}6$, 636	$\bar{1}\bar{1}$, $\bar{3}$, 9, 21, 5, $\bar{7}$	$5\bar{2}\bar{1}$, $27\bar{3}$, 352
observability criterion n ($I > n\sigma(I)$)	3.0	3.0	2.5	3.0
no. of data in refinement	3815	5167	5865	6293
no. of refined parameters	347	272/290	235/343	301/337
final R	0.023	0.028	0.048	0.035
R_w	0.029	0.032	0.056	0.044
largest remaining feature in electron density map, e Å^{-3}	+0.82 (max), −0.67 (min)	+0.78 (max), −0.68 (min)	+1.01 (max), −1.07 (min)	+1.32 (max), −1.25 (min)
shift/esd in last cycle	0.43 (max), 0.02 (av)	0.09 (max), 0.02 (av)	0.25 (max), 0.01 (av)	0.11 (max), 0.02 (av)

determined by the bonding requirements of the vinylidene ligand.

Treatment of solutions of complex **6** (prepared in situ by addition of dppe to **4**) with excess $HBF_4 \cdot Et_2O$ results in a color change from orange to red, and the formation of the alkyne complex $[Ru_3Pt(\mu\text{-}H)(\mu_4\text{-}\eta^2\text{-}CH{\equiv}C(t\text{-}Bu))(CO)_9(dppe)]^+BF_4^-$ (**18**). Protonation thus proceeds at the C_α alkynyl site. The IR spectrum in the ν_{CO} region is very similar to those of **11** and **17**, suggesting a butterfly Ru_3Pt core. The low-frequency ^{195}Pt satellites of the two ^{31}P resonances (δ 68.6 and 66.9) are fortuitously coincident at ca. δ 51. They appear as a sharp singlet at 263 K, but as a broad pair of superimposed doublets at 233 K, indicating a slow exchange of the inequivalent ^{31}P environments. The terminal alkyne proton is seen at δ 9.60 in the ^1H NMR spectrum, in the region characteristic[68] for these protons, while ^{13}C signals for the alkyne carbons occur at δ 149.1 (J(H–C) = 167 Hz) and 204.7. In the ^1H-coupled spectrum the latter resonance is broadened, due to long-range unresolved couplings to the t-Bu protons.[67] The absence of detectable ^{195}Pt couplings on the alkyne signals suggests there is no significant interaction between the Pt atom and the alkyne ligand, and we tentatively suggest the structure shown below.

It is interesting to note that, in contrast to the facile protonation of **6** at the C_α site, the related cluster $Ru_3(\mu\text{-}H)\{\mu_3\text{-}\eta^2\text{-}C{\equiv}C(t\text{-}Bu)\}(CO)_9$ undergoes protonation initially at an Ru–Ru edge, and only under forcing conditions is the C_α site protonated.[68] Solutions of **18** are unstable and undergo irreversible isomerization to **17** over a period of 12 h. The protonation reactions of **6** and **11** provide further evidence that the isomerization of **6** to **11** does not involve a deprotonation of **6**, followed by a reprotonation at the C_β alkynyl site. An intramolecular hydride migration seems the most likely route for this reaction. The transformations discussed in this paper are summarized in Scheme II.

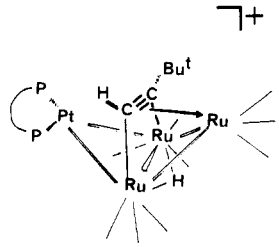

18

Experimental Section

All manipulations were carried out under dry, oxygen-free dinitrogen atmosphere, using standard vacuum line/Schlenk tube techniques. Solvents were deoxygenated and freshly distilled under dinitrogen prior to use; petroleum ether refers to that fraction with a boiling point of 40–60 °C. ^1H, ^{13}C, and ^{31}P NMR spectra were obtained on either a Varian XL100 or Bruker WP 200SY FT NMR spectrometer. Chemical shifts were referenced to internal solvent signals for ^1H and ^{13}C spectra and are reported relative to Me_4Si. ^{31}P spectra were referenced to external 85% H_3PO_4. Dynamic NMR spectra were simulated by using a locally adapted version of DNMR3.[69] NMR probe temperatures were calibrated by using the method of van Geet[70] and are considered accurate to ±2 K. Thermodynamic parameters were determined from rate data by using standard methods.[71] Infrared spectra were measured on a Perkin-Elmer 983 photospectrometer. Elemental analyses (C/H) were performed by the Microanalytical Unit in the Department of Chemistry, University of Glasgow. Column chromatography was carried out by using Florosil (BDH 100–200 mesh) in hexane using hexane or hexane/dichloromethane mixtures as eluants. $Pt(COD)_2$[72] and $Ru_3(\mu\text{-}H)(\mu_3\text{-}\eta^2\text{-}C{\equiv}C(t\text{-}$

(68) Barner-Thorsen, C.; Rosenberg, E.; Saatjian, G.; Aime, S.; Milone, L.; Osella, D. *Inorg. Chem.* **1981**, *20*, 1592.
(69) Kleier, D. A.; Binsch, G. *QCPE* **1970**, *11*, 165.
(70) van Geet, A. L. *Anal. Chem.* **1970**, *42*, 679.
(71) Sandström, J. *Dynamic NMR Spectroscopy*; Academic: New York, 1982.
(72) Spencer, J. L. *Inorg. Synth.* **1979**, *19*, 213.

Scheme II

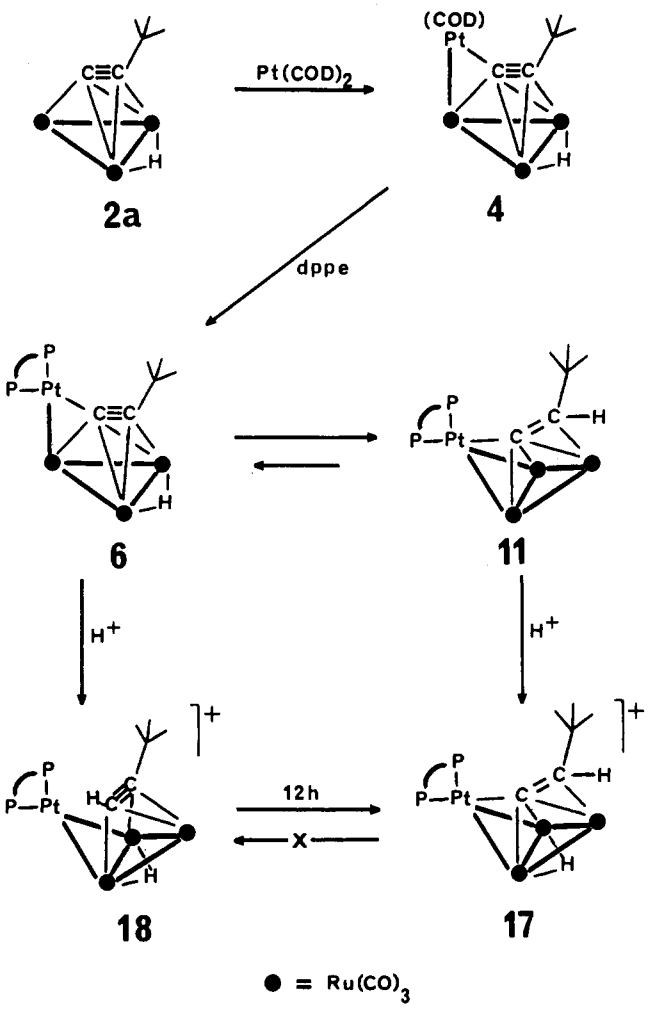

Bu))$(CO)_9$[52] were synthesized by previously reported methods. Samples of the latter complex were enriched with ^{13}CO by heating solutions in toluene for 5 days at 90 °C under an atmosphere of ^{13}CO (99% ^{13}C).

Preparation of $Ru_3Pt(\mu\text{-}H)(\mu_4\text{-}\eta^2\text{-}CC(t\text{-}Bu))(CO)_9(COD)$ (4). $Pt(COD)_2$ (0.766 g, 1.9 mmol) in toluene (5 mL) was added dropwise over a period of 10 min to a stirred solution of $Ru_3(\mu\text{-}H)(\mu_3\text{-}\eta^2\text{-}C{\equiv}C(t\text{-}Bu))(CO)_9$ (1.18 g, 1.9 mmol) in toluene (30 mL) at 0° C. The color of the solution changed from light yellow to dark red-brown over 25 min. The toluene was removed under vacuum and the residue chromatographed. After elution of unreacted starting materials, the product was eluted with hexane as a bright orange band. Removal of solvent and recrystallization from diethyl ether afforded 0.98 g (1.04 mmol) of $Ru_3Pt(\mu\text{-}H)(\mu_4\text{-}\eta^2\text{-}C{\equiv}C(t\text{-}Bu))(CO)_9(COD)$ as orange crystals: yield 56%; IR (cyclohexane) ν_{CO} 2080 (m), 2069 (vw), 2057 (s), 2023 (vs), 2006 (m), 1999 (m), 1970 (w), 1953 (w) cm^{-1}; ^1H NMR ($CD_3C_6D_5$, 233 K) δ 6.02 (s, 2 H, CH=CH, J(Pt–H) = 49 Hz), 5.28 (s, 2 H, CH=CH, J(Pt–H) = 71 Hz), 1.62 (br s, 8 H, CH_2), 1.30 (s, 9 H, t-Bu), –19.25 (s, 1 H, Ru(μ-H)Ru, J(Pt–H) = 6.4 Hz); ^{13}C NMR (CD_2Cl_2, 220 K) δ 209.4 (s, 1 C, $C{\equiv}C(t$-Bu), J(Pt–C) = 1621 Hz), 205.8 (s, 1 C, CO), 197.7 (s, 2 C, CO, J(Pt–C) = 12 Hz), 195.4 (s, 2 C, CO), 190.4 (s, 2 C, CO, J(Pt–C) = 16, J(H–C) = 13 Hz), 189.4 (s, 2 C, CO), 121.9 (s, 1 C, $C{\equiv}C(t$-Bu), J(Pt–C) = 224 Hz), 105.2 (s, 2 C, $CH{=}CH$, J(Pt–C) = 60, J(H–C) = 159 Hz), 92.4 (s, 2 C, $CH{=}CH$, J(Pt–C) = 134, J(H–C) = 155 Hz), 39.8 (s, 1 C, $C(CH_3)_3$), 32.5 (s, 3 C, $C(CH_3)_3$, J(H–C) = 125 Hz), 30.3 (s, 2 C, CH_2, J(Pt–C) = 20, J(H–C) = 122 Hz), 29.0 (s, 2 C, CH_2, J(H–C) = 127 Hz). Anal. Calcd for $C_{23}H_{22}O_9Ru_3Pt$: C, 29.36; H, 2.36. Found: C, 29.57; H, 2.06.

Reaction of 4 with Bis(diphenylphosphino)ethane. Bis(diphenylphosphino)ethane (0.110 g, 0.278 mmol) in diethyl ether (10 mL) was added to a stirred solution of complex 4 (0.261 g, 0.278 mmol) in diethyl ether (30 mL). There was an immediate color change from light orange to red. After 15 min the volatiles were removed and the residue was chromatographed. Elution with petroleum ether separated an orange band which afforded 0.102 g (0.083 mmol) of orange crystals of $Ru_3Pt(\mu\text{-}H)(\mu_4\text{-}\eta^2\text{-}C{\equiv}C(t\text{-}Bu))(CO)_9(dppe)$ (6) (30% yield) on recrystallization at –20 °C from diethyl ether: IR (cyclohexane) ν_{CO} 2073 (m), 2050 (s), 2017 (s), 1999 (m), 1987 (m), 1962 (vw), 1951 (w) cm^{-1}; ^1H NMR ($CDCl_3$, 233 K) δ 7.76–7.32 (m, 20 H, C_6H_5), 2.40–2.15 (m, 4 H, CH_2), 0.74 (s, 9 H, t-Bu), –19.12 (s, 1 H, Ru(μ-H)Ru); ^{31}P NMR ($CDCl_3$, 233 K) δ 46.5 (d, 1 P, J(P–P) = 17.3, J(Pt–P) = 4152 Hz), 51.8 (d, J(P–P) = 17.3, J(Pt–P) = 2643 Hz); ^{13}C NMR (CD_2Cl_2, 233 K) δ 228.3 (dd, 1 C, $C{\equiv}C(t$-Bu), J(P–C) = 15, 75 Hz), 207.7 (dd, 1 C, CO, J(P–C) = 4, 15 Hz), 198.5 (s, 2 C, CO), 195.3 (s, 2 C, CO, J(Pt–C) = 27 Hz), 192.4 (s, 2 C, CO, J(H–C) = 13 Hz), 189.9 (s, 2 C, CO), 134.3–128.3 (m, 24 C, C_6H_5), 123.7 (d, 1 C, $C{\equiv}C(t$-Bu), J(P–C) = 5, J(Pt–C) = 178 Hz), 39.8 (s, 1 C, $C(CH_3)_3$), 32.1 (m, 1 C, CH_2), 31.9 (s, 3 C, $C(CH_3)_3$), 28.1 (m, 1 C, CH_2). Anal. Calcd for $C_{41}H_{34}O_9P_2Ru_3Pt$: C, 40.01; H, 2.78. Found: C, 40.30; H, 2.75. On further elution with dichloromethane/petroleum ether (1:1) a red band separated which afforded 0.215 g (0.175 mmol) of red crystals of $Ru_3Pt(\mu_4\text{-}\eta^2\text{-}C{=}C(H)t\text{-}Bu)(CO)_9(dppe)$ (11) (63% yield) on recrystallization from dichloromethane/petroleum ether at –20 °C: IR (cyclohexane) ν_{CO} 2061 (s), 2018 (s), 2005 (vs), 1996 (m), 1974 (w), 1963 (w), 1951 (w) cm^{-1}; ^1H NMR ($CDCl_3$, 298 K) δ 7.82–7.23 (m, 20 H, C_6H_5), 5.75 (dd, 1 H, $C{=}CH(t$-Bu, J(P–H) = 4.5, 5.0 Hz), 2.8–1.9 (m, 4 H, CH_2), 0.56 (s, 9 H, t-Bu); ^{31}P NMR ($CDCl_3$, 243 K) δ 55.5 (J(Pt–P) = 3452 Hz) and 52.7 (J(Pt–P) = 3600 Hz) as AB pattern (J(P–P) = 19.0 Hz); ^{13}C NMR (CD_2Cl_2, 295 K) δ 319.7 (t, 1 C, $C{=}C(H)t$-Bu, J(P–C) = 27 Hz), 203.8 (s, 1 C, CO), 200.7 (s, 6 C, CO), 193 (v br s, 2 C, CO), 136.0–128.7 (m, 24 C, C_6H_5), 100.3 (s, 1 C, $C{=}C(H)t$-Bu, J(Pt–C) = 73 Hz), 39.0 (s, 1 C, $C(CH_3)$), 33.1 (s, 3 C, $C(CH_3)_3$), 29.9 (dd, 1 C, CH_2, J(P–C) = 38, 13 Hz), 25.9 (dd, 1 C, CH_2, J(P–C) = 36, 13 Hz); ^{13}C NMR (CD_2Cl_2, 171 K, ^{13}CO-enriched, carbonyl region) δ 205.4 (d, J(P–C) = 11.1 Hz), 205.2 (br), 204.2 (s), 201.1 (d, J(Pt–C) = 56, J(P–C) = 3.6 Hz), 200.6 (br), 195.6 (br), 195.1 (s), 194.1 (d, J(P–C) = 2.9 Hz), 192.2 (d, J(P–C) = 3.2 Hz). Anal. Calcd for $C_{41}H_{34}O_9P_2Ru_3Pt$: C, 40.01; H, 2.78. Found: C, 40.37; H, 2.74.

Reaction of 4 with CO. CO was bubbled through a solution of 4 (0.05 g) in CH_2Cl_2 (5 mL) for 5 min. The solution turned dark brown in color and deposited a brown purplish material ca. 0.01 g. The mother liquor contained complex **2a** as determined from IR spectra. Data on brown material: IR (KBr disk) 2053 (vs), 1882 (s), 1822 (m), 474 (w), 405 (w) cm^{-1}. Anal. Found: C, 2.0; H, 0.0.

Preparation of $[Ru_3Pt(\mu\text{-}H)(\mu_4\text{-}\eta^2\text{-}C{=}C(H)t\text{-}Bu)(CO)_9(dppe)]^+BF_4^-$ (17). An excess of $HBF_4{\cdot}Et_2O$ was added to a solution of complex 11 (0.15 g, 0.12 mmol) in CH_2Cl_2 (10 mL) resulting in a yellow solution. Addition of diethyl ether (ca. 10 mL) precipitated bright orange crystals of $[Ru_3Pt(\mu\text{-}H)(\mu_4\text{-}\eta^2\text{-}C{=}C(H)t\text{-}Bu)(CO)_9(dppe)]^+BF_4^-$ (17): 0.14 g, 0.11 mmol, 92% yield; IR (CH_2Cl_2) ν_{CO} 2095 (s), 2071 (vs), 2059 (s), 2032 (m), 2023 (m), 2000 (w, sh) cm^{-1}; ^1H NMR (CD_2Cl_2, 295 K) δ 7.9–7.27 (m, 20 H, C_6H_5), 5.72 (t, 1 H, $C{=}C(H)t$-Bu, J(P–H) = 4.7 Hz), 2.8–2.0 (m, 4 H, CH_2), 0.77 (s, 9 H, t-Bu), –20.34 (t, 1 H, Ru(μ-H)Ru, J(Pt–H) = 13, J(P–H) = 2.9 Hz); ^{31}P NMR (CD_2Cl_2, 298 K) δ 55.1 (d, J(Pt–P) = 3345 Hz), 53.2 (d, J(Pt–P) = 3448 Hz) as AB pattern (J(P–P) = 19.0 Hz); ^{13}C NMR (CD_2Cl_2, 298 K) δ 303.5 (dd, 1 C, $C{=}C(H)t$-Bu, J(P–C) = 28,23 Hz), 136.3–127.6 (m, 24 C, C_6H_5), 100.2 (s, 1 C, $C{=}C(H)t$-Bu, J(Pt–C) = 73 Hz), 39.8 (s, 1 C, $C(CH_3)_3$), 33.6 (s, 3 C, $C(CH_3)_3$), 30.7 (dd, 1 C, CH_2, J(Pt–C) = 50, J(P–C) = 28, 10 Hz), 26.9 (dd, 1 C, CH_2, J(Pt–C) = 39, J(P–C) = 38, 11 Hz); $^{13}C\{^1H\}$ NMR (CD_2Cl_2, 242 K, ^{13}CO-enriched, carbonyl region) δ 197.5 (s, J(Pt–C) = 12 Hz), 193.9 (d, J(P–C) = 10.4, J(H_1–C) = 3.5 Hz), 193.7 (d, J(P–C) = 11.9, J(H_1–C) = 3.0 Hz), 190.9 (s, J(Pt–C) = 7, J(H_1–C) = 13.2 Hz), 190.6 (d, J(P–C) = 2.0, J(H_{12}–C) = 5.0 Hz), 189.8 (s, J(H_1–C) = 15.1 Hz), 189.1 (d, J(P–C) = 2.3 Hz), 188.9 (d, J(Pt–C) = 44, J(H_1–C) = 4, J(P–C) = 5.2 Hz), 187.9 (d, J(Pt–C) = 52, J(H_1–C) = 4.0, J(P–C) = 3.3 Hz). Anal. Calcd for $C_{41}H_{35}BF_4O_9P_2PtRu_3$: C, 37.34; H, 2.68. Found: C, 37.32; H, 2.67.

Preparation of $[Ru_3Pt(\mu\text{-}H)(\mu_4\text{-}\eta^2\text{-}CH{\equiv}C(t\text{-}Bu))(CO)_9(dppe)]^+BF_4^-$ (18). To a solution of complex 4 (0.1 g, 0.11 mmol) in CH_2Cl_2 (10 mL) was added an equimolar amount of dppe (this reaction mixture contains essentially pure, >95%, complex 6), and then after ca. 1 min an excess of $HBF_4{\cdot}Et_2O$. Careful addition

of petroleum ether affords the orange microcrystalline $[Ru_3Pt(\mu\text{-}H)(\mu_4\text{-}\eta^2\text{-}CH{\equiv}C(t\text{-}Bu))(CO)_9(dppe)]^+BF_4^-$ (18): 0.12 g, 0.09 mmol, 82% yield; IR (CH_2Cl_2) ν_{CO} 2090 (m), 2070 (vs), 2052 (s), 2034 (w), 2016 (m), 2005 (w, sh) cm^{-1}; ^1H NMR ($CDCl_3$, 298 K) δ 9.60 (s, 1 H, ≡CH), 8.0–7.1 (m, 20 H, C_6H_5), 3.07 (br m, 2 H, CH_2), 2.10 (br m, 2 H, CH_2), 1.27 (s, 9 H, *t*-Bu), −19.18 (t, 1 H, Ru(μ-H)Ru, J(P–H) = 4.0 Hz); ^{31}P NMR (CD_2Cl_2, 263 K) δ 68.6 (d, J(Pt–P) = 2939 Hz), 66.9 (d, J(Pt–P) = 2663 Hz) as AB pattern (J(P–P) = 19 Hz); ^{13}C NMR (CD_2Cl_2, 265 K) δ 211.1 (s, 1 C, CO), 204.7 (s, 1 C, HC≡*C*-*t*-Bu), 194.3–192.3 (overlapping mult, 4 C, CO), 190.2–188.5 (overlapping mult, 3 C, CO), 186.1 (s, 1 C, CO, J(H–C) = 11 Hz), 149.1 (s br, 1 C, *C*H≡C-*t*-Bu, J(H–C) = 167 Hz), 135.4–125.9 (m, 24 C, C_6H_5), 45.5 (s, 1 C, $C(CH_3)_3$), 33.3 (s, 3 C, $C(CH_3)_3$), 31.4 (dd, 1 C, CH_2, J(P–C) = 12, 38 Hz), 24.7 (dd, 1 C, CH_2, J(P–C) = 13, 36 Hz). Anal. Calcd for $C_{41}H_{35}BF_4O_9P_2PtRu_3$: C, 37.34; H, 2.68. Found: C, 37.40; H, 2.32%.

Kinetic Experiments. Samples in $CDCl_3$ were thermostated at 296 (±1) K, and the relative concentrations of **6** and **11** were determined at regular intervals from integration of the *t*-Bu signals (assuming equal T_1's) in the ^1H NMR spectra (64 transients, 10-s relaxation delay, 200 MHz). Initial concentrations of the three samples were (a) complex **6**, 0.017 M, (b) complex **6** 0.0173 M, with NEt_3, 0.019 M, and (c) complex **6**, 0.0189 M, with pyridine, 0.052 M. Rate constants were obtained from a least-squares fit to the data points. Equilibrium concentrations of **6** and **11** were measured after 5 days, after which time no signals other than those of **6** and **11** were detectable.

Reaction of Complex 11 with Dihydrogen. A solution of **11** (0.1 g) in cyclohexane (100 mL) was refluxed under a dihydrogen purge for 3 h. The solution darkened considerably over this time. IR spectra taken at regular intervals showed only the presence of unreacted **11**, and no tractable products were obtained.

Crystal Structure Determinations. Crystals of **4** were grown from petroleum ether, **6** from diethyl ether, **11** from cyclohexane, and **17** from CH_2Cl_2/diethyl ether mixture. Details of data collection procedures and structure refinement are given in Table X. Data were collected on an Enraf-Nonius CAD4F automated diffractometer, with graphite-monochromated X-radiation (λ = 0.710 69 Å). Unit cell parameters were determined by refinement of the setting angles ($\theta \geq 12°$) of 25 reflections. Data were collected at 298 K by using the $\theta/2\theta$ scan mode, and standard reflections were measured every 2 h during data collection. No decay correction was deemed necessary for complexes **4** and **17**, while linear decay corrections were applied to the data sets of **6** and **11**, corresponding to decays of 3.3 and 8.4% respectively, over 10 000 data. Lorentz–polarization and absorption (DIFABS[73]) corrections were applied to all data sets. Systematic absences uniquely determined the space group $P2_1/n$ for complexes **4** and **6** and indicated the space groups $C2/c$ (or Cc) and $P\bar{1}$ (or $P1$) for **11** and **17**, respectively. E statistics favored centrosymmetric space groups for these latter complexes. These choices were confirmed by the successful solution and refinement of all structures. Structures were solved by direct methods (MITHRIL[74]) and subsequent electron density difference syntheses. All non-hydrogen atoms, except for the phenyl carbon atoms in complexes **11** and **17**, were allowed anisotropic thermal motion. Hydride positions were obtained from difference Fourier maps, as were the olefinic hydrogens in complex **4** and the vinylidene hydrogen for complex **17**. All other hydrogen atoms were included at calculated positions, assuming a C–H bond length of 1.0 Å. No hydrogen positional parameters were refined. For complexes **6**, **11**, and **17** hydrogen atom isotropic thermal parameters were fixed at 0.05 or 0.08 $Å^2$, while these parameters were refined for **4**. Refinement was by full-matrix least squares. Due to matrix-size limitations parameters were divided into blocks and each was refined separately. The function minimized was $\sum w(|F_o| - |F_c|)^2$ with the weighting scheme $w = [\sigma^2(F_o)]^{-1}$ used and judged satisfactory. $\sigma(F_o)$ was estimated from counting statistics. Neutral atom scattering factors were taken from ref 75 with corrections applied for anomalous dispersion. All calculations were carried out on a Gould-SEL 32/27 mini computer using the GX suite of programs.[76]

Acknowledgment. We thank the SERC for a research studentship (to P.E.) and Johnson-Matthey for a generous loan of Pt and Ru salts. Professor H. Vahrenkamp is thanked for a preprint of ref 23.

Note Added in Proof. The preparation and crystal structure of the triiron platinum cluster $Fe_3Pt(\mu_4\text{-}\eta^2\text{-}C{=}C(H)Ph)(CO)_9(dppe)$, which is closely related to complex **11**, has been briefly reported by Soviet workers; see: Kovalenko, S. V.; Antonova, A. B.; Deikhina, N. A.; Ioganson, A. A.; Korniets, E. D.; Ginzburg, A. G.; Yanovskii, A. I.; Slovokhotov, Yu. L.; Struchkov, Yu. T. *Izv. Akad. Nauk SSSR, Ser. Khim.* **1987**, *12*, 2864.

Registry No. **2a**, 57673-31-1; **4**, 119593-13-4; **6**, 119593-14-5; **11**, 119567-03-2; **17**, 119567-05-4; **18**, 119593-16-7; $Pt(COD)_2$, 12130-66-4; Pt, 7440-06-4; Ru, 7440-18-8.

Supplementary Material Available: Tables of anisotropic thermal parameters and calculated hydrogen positional parameters and complete listings of bond lengths and angles (27 pages); listings of calculated and observed structure factors (101 pages). Ordering information is given on any masthead page.

(73) Walker, N.; Stuart, D. *Acta Crystallogr., Sect. A: Found. Crystallogr.* **1983**, *A39*, 158.

(74) Gilmore, C. J. *J. Appl. Cryst.* **1984**, *17*, 42.

(75) *International Tables for X-Ray Crystallography*; Kynoch: Birmingham, 1974; Vol. 4.

(76) Mallinson, P. R.; Muir, K. W. *J. Appl. Cryst.* **1985**, *18*, 51.